

1 **Summer greenhouse gas fluxes in different types of hemiboreal lakes**

2

3 **Author names and affiliations.**

4 Eva-Ingrid Rõõm^{a,b,1}, Velda Lauringson^{a,c,1}, Alo Laas^a, Kersti Kangro^{a,d}, Malle Viik^a, Pille
5 Meinson^a, Fabien Cremona^a, Peeter Nõges^a, Tiina Nõges^a

6 ^a Chair of Hydrobiology and Fishery, Institute of Agricultural and Environmental Sciences,
7 Estonian University of Life Sciences, Kreutzwaldi 5, 51006 Tartu, ESTONIA

8 ^b Environmental Investment Centre, Narva mnt 7A, 15172 Tallinn, ESTONIA

9 ^c Institute of Ecology and Earth Sciences, Faculty of Science and Technology, University of
10 Tartu, Vanemuise Str 46, 51014 Tartu, ESTONIA

11 ^d Tartu Observatory, Faculty of Science and Technology, University of Tartu,
12 Observatooriumi 1, Tõravere, Nõo parish, 61602, Tartu County, ESTONIA

13

14 **Corresponding author.**

15 E-mail address: velda.lauringson@gmail.com (Velda Lauringson)

16 ¹ These authors share the co-first author position

17

18 Abstract

19 Lakes are considered important regulators of atmospheric greenhouse gases (GHG). We
20 estimated late summer open water GHG fluxes in nine hemiboreal lakes in Estonia classified under
21 different lake types according to the European Water Framework Directive (WFD). We also used the
22 WFD typology to provide an improved estimate of the total GHG emission from all Estonian lakes
23 with a gross surface area of 2204 km² representing 45,227 km² of hemiboreal landscapes (the territory
24 of Estonia). The results demonstrate largely variable CO₂ fluxes among the lake types with most
25 active emissions from Alkalitrophic (Alk), Stratified Alkalitrophic (StratAlk), Dark Soft and with
26 predominant binding in Coastal, Very Large, and Light Soft lakes. The CO₂ fluxes correlated strongly
27 with dissolved CO₂ saturation (DCO₂) values at the surface. Highest CH₄ emissions were measured
28 from the Coastal lake type, followed by Light Soft, StratAlk and Alk types; Coastal, Light Soft and
29 StratAlk were emitting CH₄ partly as bubbles. The only emitter of N₂O was the Alk type. We
30 measured weak binding of N₂O in Dark Soft and Coastal lakes, while in all other studied lake types,
31 the N₂O fluxes were too small to be quantified. Diversely from the common viewpoint of lakes as net
32 sources of both CO₂ and CH₄, it turns out from our results that at least in late summer, Estonian lakes
33 are net sinks of both CO₂ alone and the sum of CO₂ and CH₄. This is mainly caused by the
34 predominant CO₂ sink function of Lake Peipsi forming ³/₄ of the total lake area and showing negative
35 net emissions even after considering the Global Warming Potential (GWP) of other GHGs. Still, by
36 converting CH₄ data into CO₂ equivalents, the combined emission of all Estonian lakes (8 T C day⁻¹)
37 is turned strongly positive: 2720 T CO₂ equivalents per day.

38

39

40 Keywords

41 Estonian GHG emission, CO₂, CH₄, N₂O, EU Water Framework Directive lake types, floating
42 chamber FTIR measurement

43 1. Introduction

44 In the world fighting against climate warming, there are still many open questions about
45 greenhouse gas (GHG) emissions from natural sources. One of the less explored areas among others is
46 the emission of the three important GHGs – carbon dioxide (CO₂), methane (CH₄), and nitrous oxide
47 (N₂O) – from lakes. There are around 117 million lakes on the globe and even though they represent
48 only a tiny fraction of the Earth's nonglaciaded land area (Verpoorter et al., 2014), they are an
49 important part of global carbon (C) and nitrogen (N) cycles. Lakes receive C and N from terrestrial
50 ecosystems and fix these elements also from the atmosphere. Both elements are sequestered and/or
51 released from lakes at various rates and in various forms depending on multiple lake characteristics
52 and processes that ultimately determine the GHG balance (Galloway et al., 2003; Tranvik et al., 2009;
53 Kortelainen et al., 2013; Wang et al., 2021). GHGs have various sources and sinks within lakes: CO₂
54 is received from the catchment under the form of dissolved or particulate inorganic carbon, from
55 atmosphere, and it is released in the course of organic matter decomposition through within-lake
56 pelagic and benthic respiration (Del Giorgio et al., 1999). Depending on the partial pressure in the
57 lake's surface layer, CO₂ may either outgas from the lake or be absorbed from the atmosphere through
58 the water-air interface. Water carbonate and humic substance concentrations are important in
59 predicting the dissolved CO₂ (DCO₂) levels in lakes (Karlsson et al., 2007; Marcé et al., 2015; Khan
60 et al., 2022). Diversely, CH₄ is mostly created within lakes and never absorbed from the atmosphere,
61 as this gas is almost always supersaturated in lakes relative to the atmosphere (Bastviken et al., 2004).
62 The major part of CH₄ is produced by methanogenic microbes in the anoxic zone of organic-rich
63 sediments (Bastviken et al., 2004). Still, as the surface layer of lakes is often supersaturated with CH₄,
64 it has been hypothesized that efficient source processes should also exist in the oxic pelagic zone
65 (Bogard et al., 2014). The surface CH₄ pool, however, may also be supplied by an advective transport
66 from the shallow water macrophyte beds which support considerably high rates of conventional
67 benthic methanogenesis due to their very high production and burial rates of organic matter (Juutinen
68 et al., 2003; Kankaala et al., 2005). In addition to diffusional flux from the sediments, CH₄
69 supersaturation in sediments may lead to bubble formation and subsequent release, which is especially

70 frequent under shallow water column due to low hydrostatic pressure, and it may also be released to
71 the atmosphere through the stems of vascular plants (Whiting and Chanton, 1996; Bastviken et al.,
72 2004). The third aforementioned gas, N_2O , is created in lakes mostly during microbial nitrification or
73 ammonification as a by-product and in denitrification as an intermediate product (Knowles, 1982).
74 Consequently, its source may be either ammonia excreted or degraded from organic matter or nitrates
75 acquired from the atmosphere or catchment runoff, the latter also via groundwater.

76 All the three gases are also quickly consumed in lakes – CO_2 is fixed by various guilds of
77 autotrophs all over the water column (Lapierre et al., 2017) while CH_4 is actively consumed by either
78 anoxic or oxic methanotrophs in redoxclines or the oxic zone, respectively (Bodelier and Steenbergh,
79 2014). Methane captured in bubbles or released through plant stems, nevertheless, escapes
80 methanotrophy (Langenegger et al., 2019). For N_2O , the only known sink is the last step of
81 denitrification pathway, which in case of classical denitrification takes place in reduced environment
82 in the absence of oxygen and at depleted nitrates (Chapuis-Lardy et al., 2007, Richardson et al.,
83 2009). However, recent research has found that an aerobic N_2O reduction may be widespread in soils
84 and oceans, carried out by non-denitrifying microbes possessing a previously unknown type of N_2O
85 reductase gene and commonly lacking enzymes for the preceding steps in the denitrification reaction
86 chain (Sanford et al., 2012; Rees et al., 2021).

87 While lakes are increasingly viewed as hotspots for CO_2 and CH_4 emissions, their
88 contribution to N_2O emissions is considered negligible compared to terrestrial ecosystems (Tranvik et
89 al., 2009). Even more, certain types of lakes may at least periodically be important consumers of N_2O
90 (Webb et al., 2019) and may have historically been so even more before the era of intense agricultural
91 use of nitrogen fertilizers. The conditions potentially favouring N_2O reduction – abundant labile
92 organic matter coupled with the temporary shortage of oxidised nitrogen – can be easily met in these
93 waterbodies (Knowles, 1982).

94 The global estimates of GHG emissions from lakes build on the extrapolation of average rates
95 of emissions related to lake size or other widely measured characteristics and the density distributions
96 of lakes along the gradients of these characteristics (Downing, 2009). The best global estimates to

97 date have taken account of both the size of the lakes and some available predictor variables for
98 productivity such as nutrients and surface water chlorophyll *a* (Chl *a*) content (DelSontro et al., 2018).
99 However, there is a range of other potentially important predictors of lake GHG fluxes like depth,
100 spatial coverage of macrophytes, the stability of stratification, water pH, concentrations of dissolved
101 salts, organic and inorganic carbon, and volcanism, to name a few (Bastviken et al., 2004; Kankaala et
102 al., 2013; Andrade et al., 2016, 2019a; Davidson et al., 2018). Data on these predictors, while lacking
103 at the global scale, may however be available at a regional scale. Several studies have revealed
104 patterns related to environmental gradients and/or some categorization of waterbodies (e.g. lakes and
105 ditches in Netherlands; ponds, reservoirs, and lakes in Canada) (Schrier-Uijl et al., 2011; Tadonl  k   et
106 al., 2011; DelSontro et al., 2016). For instance, trophic state, alkalinity, humic substances,
107 stratification, and temperature have all emerged as good predictors for pelagic emissions in boreal
108 and/or temperate lakes in North America and Europe (Schrier-Uijl et al., 2011; Marc   et al., 2015;
109 Weyhenmeyer et al., 2015; Yang et al., 2015; DelSontro et al., 2016; Webb et al., 2019). Some studies
110 from Sweden and Finland have further provided regional estimates for lakes based on water chemistry
111 and/or some physical characteristics like lake size and water retention time (Kortelainen et al., 2006;
112 Kankaala et al., 2013; Weyhenmeyer et al., 2015). Tank et al. (2009) estimated the CO₂ fluxes of the
113 Mackenzie River Delta area lakes (Canadian Arctic) based on three lake types describing the degree
114 of isolation of lakes from the watershed. However, we are not aware, for regional extrapolations, of
115 any utilization of elaborate composite categorizations (typologies) which are adjusted for monitoring
116 purposes and group lakes based on combination of several factors, despite such systems are widely
117 used for the management of anthropogenic disturbances and are in many cases very finely tuned
118 (Moss et al., 2003; N  ges et al., 2007). National or regional lake typologies based on water chemistry
119 and morphometric features (*e.g.* as the one established by the European Union Water Framework
120 Directive (WFD)) would allow to improve the estimates of aquatic GHG emissions. Knowing the
121 conditions in different lake types and the type-specific areal net GHG emissions enables (1) to raise
122 strong hypotheses in order to find out the biogeochemical processes responsible for the emissions in
123 particular lakes; (2) to design type-specific mitigation measures based on these processes; (3) to

124 prioritise the management measures depending on the areal proportion of different lake types in a
125 region, e.g., it may be easier to manage large emissions from lakes with a small area than vice versa.

126 The aims of the present study were (1) to create the first inventory of lake type specific
127 summer GHG fluxes in the pelagic zone of hemiboreal Estonian lakes according to the WFD lake
128 types (Table 1), (2) to study the connections between GHG emissions and lake physico-chemical and
129 biological parameters, and (3) to compile a regional assessment of GHG emissions from lakes
130 considering the areal distribution of lakes between the different lake types. We mapped GHG fluxes
131 of nine lakes representing the different type classes and hypothesised largely variable type specific
132 GHG emissions. We further extrapolated from our results an estimate of late summer GHG fluxes
133 from all Estonian lakes with a gross surface area of 2204 km².

134

135 **2. Study area characterization**

136 **2.1 Lake typology**

137 All studied lakes (Fig. 1, A – I) were chosen to be typical representatives of the eight Estonian
138 lake types according to the WFD typology, which is based on lake area, alkalinity, conductivity,
139 chloride content, thermal stratification, and colour (Table 1). The two largest lakes in Estonia, Peipsi
140 (Peipus, 3555 km², the fifth largest lake in Europe) and Võrtsjärv (270 km²), form individual types
141 referred to as V-Large and Large (Fig. 1, A – B). They were allocated to separate lake types in the
142 WFD compliant lake typology (ME, 2020) because strong wind induced mixing makes them
143 incomparable with smaller lakes in the region, whereas stronger sediment resuspension in the
144 shallower Võrtsjärv causes higher turbidity and light limitation clearly distinguishing it from the
145 deeper Peipsi.

146 The remaining 2534 small lakes are grouped into six types (Ott, 2006; ME, 2020). For our
147 study purposes, we created a ninth lake type – the stratified alkalitrophic lakes (StratAlk) – to account
148 for the potential differences in GHG emissions. To make the text easier to follow, the nine lakes in
149 this study are further referred to by their abbreviated type names (Table 1 and Fig. 2).

150 A general overview of the most important lake parameters is given in Table 2. All lakes were

151 rather shallow with a mean depth below 10 m. Measurements in all lakes were carried out within a 2-
152 month period from July to September 2014 (Table 3), and measurements of CO₂ and CH₄ fluxes
153 above the lakes with all supportive physicochemical measurements were made once or twice during
154 the same period.

155 **2.2 Alkalitrophic lakes (Alk)**

156 The study lake, Äntu Sinijärv, is a source lake fed by karstic ground waters and represents
157 highly alkalitrophic (>240 HCO₃⁻ mg L⁻¹) lakes in Estonia (Fig. 1C). Lakes of this type are
158 characteristic of the Pandivere Upland area (only a few elsewhere) and with a total area of ca 200 ha
159 they make up only 0.09% of the total area of lakes in Estonia (EDR – *environmental data register of*
160 *Estonia*). With a mean light attenuation coefficient (K_d) of $0.16 \pm 0.02 \text{ m}^{-1}$ for the photosynthetically
161 active spectral region measured in 1995–96, Äntu Sinijärv was the most transparent lake in Estonia
162 (Nõges and Nõges, 1998; Nõges, 2000).

163 **2.3 Stratified alkalitrophic lakes (StratAlk)**

164 In the WFD compliant lake typology (ME 2020), these lakes are categorised under stratified
165 lakes with medium alkalinity (StratMedAlk). Considering the different character of many dimictic
166 stratified lakes with high alkalinity (>240 HCO₃⁻ mg L⁻¹), mainly located in South-East Estonia, we
167 created a new type and selected Lake Karijärv (Fig. 1D) as the representative for those 114 lakes.
168 Karijärv is a highly alkalitrophic stratified light-coloured eutrophic system in generally good
169 ecological state. During the thermal stratification from June to September, anoxia is formed at the
170 bottom despite rather high water transparency in the epilimnion (Secchi depth ca 4 m).

171 **2.4 Non-stratified lakes with medium alkalinity (MedAlk)**

172 This is the most abundant type of small lakes in Estonia, comprising approximately 1/5 of the
173 total number and 4% of the total area of lakes in this country. Lakes under this type are relatively
174 shallow, with medium water retention times and may exhibit only episodic thermal stratification.
175 Most of the lakes are eutrophic or hypertrophic. Lake Ülemiste, selected as the study site (Fig. 1G),
176 provides drinking water for Estonian capital city Tallinn (0.43 mln people).

177 **2.5 Stratified lakes with medium alkalinity (StratMedAlk)**

178 The 201 lakes of this type, represented in our study by Lake Saadjärv (Fig. 1H), form 2.3% of
179 the total lake area making it the second most abundant small lake type in Estonia. Being deeper, these
180 lakes provide more diverse habitats than the non-stratified lakes but are also more sensitive to human
181 impacts due to the potential build-up of bottom anoxia, leading to sediment phosphorus release and
182 thus a positive feedback to eutrophication (Ott, 2010).

183 **2.6 Dark-coloured soft-water lakes (DarkSoft)**

184 By area, about 1.5% of Estonian lakes are dark-coloured soft-water lakes (890 lakes). These
185 lakes are shallow and acidic containing large amounts of humic matter that contributes to radiative
186 heating in summer (Ott, 2010). Strong light attenuation (up to 11 m^{-1}) restricts the euphotic layer and
187 limits photosynthesis (Reinart et al., 2000). In our study, this lake type is represented by Valguta
188 Mustjärv, a very shallow 20-ha lake that has partly recovered from a heavy nutrient loading in the
189 1980s (Fig. 1E).

190 **2.7 Light-coloured soft-water lakes (LightSoft)**

191 The study of Ott and Kõiv (1999) shows that the 310 light-coloured soft-water lakes comprise
192 a little more than 0.8% of all Estonian lakes by area. Those lakes have originally been oligotrophic or
193 semi-dystrophic, mainly characterised by low productivity, small catchment area implying slow water
194 exchange, low buffering capacity, and weak stress tolerance (Ott, 2010). Because of high water
195 transparency, these lakes do not develop stable stratification. If impacted, *e.g.* by eutrophication, the
196 ecosystems of light-coloured soft-water lakes become strongly destabilized, characterised by frequent
197 algal blooms and onset of stratification. In the current study, this lake type is represented by Lake
198 Erastvere (Fig. 1F).

199 **2.8 Coastal lakes (Coastal)**

200 The 221 coastal lakes constitute approximately 1.6% of the total lake area in Estonia. Their
201 functioning depends strongly on the irregular marine water inflow, which creates highly variable
202 conditions and unstable biota. Estonian coastal lakes are shallow with high pH, transparent water (to
203 the bottom) and high water temperature in summer. The main primary producers are charophytes and

204 not phytoplankton. Since those lakes are shallow and clear-water, there is no temperature
205 stratification. In our study, this category is represented by Lake Mullutu Suurlaht (Fig. 1I).

206 3. Methods

207 3.1 Greenhouse gas flux experiments

208 The gas flux was measured on two days (with the exception of Large) within the summer
209 stratification period, from July to September 2014 (Table 3) *in situ* using floating chamber combined
210 with a computer-operated portable Fourier transform infrared (FTIR) spectrometer Gasmeter Dx-4030
211 (Gasmeter Technologies Oy), also described in Rõõm *et al.* (2014). Measurements took place at one
212 precise location of each lake (Table 3), chosen to represent the open-water area. The deepest area of
213 the lake was chosen except for Large and V-Large. In Large, the measurement site was located close
214 to the long-term monitoring point which, according to Nõges and Tuvikene (2012), is representative
215 for 90% of the lake area. In V-Large, measurements were made at a station in the Mustvee bay,
216 approximately 1 km from the western shore. This station represents the characteristic depth for the
217 open-water area and is located at the downwind side of the open lake areas for most of the time.

218 Transparent rectangular polycarbonate floating chamber with a volume of 31 L was used for
219 this study. The chamber was surrounded by an isolation foam tube to achieve chamber buoyancy.
220 Foam frames were equipped with stabilizing weights (around 6 kg) to withstand wave action during
221 windy conditions common especially in large lakes. The chamber and FTIR spectrometer were
222 connected with teflon tubes and the air was pumped through the 0.4-L sample cell of the spectrometer
223 with a constant speed of 2 L min⁻¹. Rotation of the air was found to be sufficient and no fans were
224 added to the chamber. The temperature in the chamber did not differ more than ± 5 °C from the
225 ambient air temperature, guaranteeing a less than 2% concentration difference in the chamber caused
226 by temperature. The spectrometer was calibrated with pure gaseous nitrogen (AGA, 5.0 N₂) for the
227 baseline correction once before every measuring day and, if needed, repeatedly during the day. The
228 results (average of 10 measured spectra per minute) were collected automatically within 1-min
229 interval for at least 3 min for achieving the gas concentrations of ambient air and for at least 8 min
230 from the chamber above the water. For each site, according to the consistency of the measured results,

231 two or more consecutive measurements were performed (following the method described by
232 Tremblay et al., 2005). The minimal time span spent on a single experimental site typically ranged
233 between 45 to 60 min. The concentrations of CO₂, CH₄, and N₂O as well as water vapour were
234 automatically calculated for each measured spectrum by applying the calibration datasets of IR-
235 spectra (in FTIR gas analyser database) and background calibration spectra. According to the manual,
236 the detection limit of the spectrometer Gaset Dx-4030 for N₂O is 0.02 ppm, for CH₄ 0.06 ppm, and
237 for CO₂ 11 ppm, and the linearity deviation is <2% of the measuring range. Typical volumetric
238 concentrations of the three gases in ambient air (Table 3) were, accordingly, 0.28-0.31, 1.73-2.11, and
239 369–382 ppm.

240 **3.2 Measurement of environmental variables**

241 **3.2.1 Manual measurement and sampling**

242 The set of variables measured at each floating chamber sampling occasion (Table 3) included
243 air pressure, local wind speed and direction, temperatures in the open air and floating chamber,
244 temperature profile of 0.5 m resolution down from the water surface layer (10–15 cm) to the sediment
245 top layer (at 2–3 cm depth), water and sediment pH, concentration of dissolved oxygen (DO) in water
246 as well as the depth of the water column. Air pressure was measured automatically by Gaset Dx-
247 4030. Air temperature, local wind speed and direction were measured 1 m above the water surface
248 with a HD2303.0 anemometer (DeltaOhm S.r.L.) by averaging the results of 5 equally distributed 1-
249 min measurements within a period of at least 30 min. Temperature in the floating chamber was
250 measured with a thermometer DM-9231A (Transfer Multisort Elektronik Sp. z o.o.). For field
251 measurements of DO, pH and temperature in water and sediments we used a handheld
252 multiparametric sonde (YSI ProPlus).

253 Water samples for laboratory analyses of dissolved organic carbon (DOC), phosphates (PO₄-
254 P), nitrates (NO₃-N), sulphates, chlorides, silicium, ammonium (NH₄-N), total phosphorus (TP) and
255 nitrogen (TN), carbonate alkalinity (HCO₃⁻), Chl *a*, and phytoplankton were taken from all studied
256 lakes once during the sensor deployment period. DOC concentration was measured in Whatman GF/F
257 filtrate according to Toming et al. (2013). Total phosphorus (TP) was determined with C. Zeiss

258 spectrophotometer, according to Estonian national standard EVS-EN 1189, total nitrogen (TN) with
259 Bran + Luebbe autoanalyser, according to EVS-EN ISO 13395. HCO_3^- was determined
260 colorimetrically using 0.02% methyl orange test. For Chl *a*, 0.1–1 L of water was passed through
261 Whatman GF/F glass microfiber filter and concentrations were measured spectrophotometrically in
262 96% ethanol extracts at a wavelength of 665 nm (Edler, 1979). The phytoplankton was fixed with
263 Lugol's solution and maintained in darkness until microscopic analysis. Phytoplankton cells were
264 counted and measured with an inverted microscope (Ceti Versus, Kontich-Antwerp, Belgium) at 100×
265 or 400× magnification using Utermöhl (1958) technique. Samples were counted until at least 400
266 counting units (filaments, cells, colonies), which gives a counting error of $\pm 10\%$ for the total biomass.

267 **3.2.2 Sensor deployments and monitoring stations**

268 All lakes were equipped with a high frequency monitoring platform or small lake buoy
269 (OMC-7012 data-buoy) for a 6 to 12 full days period to register changes of water temperature, DO,
270 and DCO_2 in every 10 to 30 min over the study period. Before sensor deployment, water temperature
271 (T, °C), DO, and electrical conductivity profiles were measured with handheld multiparametric sonde
272 (YSI ProPlus) to determine the location of the metalimnion from water temperature profile according
273 to Wetzel (2001). Continuous monitoring of DO concentration and water temperature was performed
274 by an automated station equipped with a multiparametric sonde (Yellow Springs Instruments (YSI)
275 66,002–4) at one-meter depth. Additional sensors for DO/temperature (Ponsel OPTOD) and for
276 dissolved CO_2 partial pressure (pCO_2) (AMT Analysenmesstechnik GmbH) were deployed at up to
277 four depths. In all lakes, the upper sensors were placed at 0.5 m depth and the position of other
278 sensors was decided depending on stratification to adequately characterize all different layers. In the
279 deepest lake (StratMedalk), a chain of 12 HOBO Pendant temperature loggers was used reaching from
280 0.5 to 20 m depth. Detailed information on high frequency data collection is given in Laas et al., 2016.
281 Automated stations were placed near the GHG flux measurement points. In DarkSoft, we
282 could not capture parallel data on CO_2 and GHG fluxes because of malfunctioning of devices. Thus,
283 for this lake, we chose close dates with similar weather conditions and used the recordings of DCO_2
284 from these days for the comparison of fluxes with DCO_2 . In MedAlk, parallel measurements of both

285 gases at all depths succeeded for one full day only. In StratMedAlk with a maximum depth of 25 m
286 we could measure temperature down to 20 m and CO₂ only down to 10 m depth due to the limited
287 length of the cables. The lake was stratified with the largest drop in pH (0.4-0.5 units) and DO (5.3-
288 6.6 mg L⁻¹) between 6 and 7 m on July 19th and between 8 and 9 m on July 26th. Below oxycline, DO
289 remained relatively stable and fluctuated by less than 2 mg L⁻¹ in every 5 m depth interval while pH
290 decreased towards bottom by ≤ 0.2 units per 5 m. Temperature drop was the largest (~8°C) between 8
291 and 15 m depth and only 0.4 °C between 15 and 20 m. For those reasons we assume that the limited
292 length of sensor cables did not affect our conclusions.

293 **3.3 Theory and calculation methods**

294 **3.3.1 Greenhouse gas flux calculations**

295 Temperature and air pressure corrections were made automatically by Gasmeter Dx-4030
296 software. Gas fluxes were calculated from linear regression of the gas concentrations in the chamber
297 headspace versus time according to Eq. (1):

$$298 \quad Flux = \frac{Slope * V}{S}$$

299 (1)

300 where *Flux* denotes GHG flux in ppm(v) C m⁻² day⁻¹, *Slope* – slope of the GHG concentration
301 in the chamber headspace versus time in ppm(v) day⁻¹, *V* – volume of air trapped in the chamber (m³),
302 and *S* – surface area of the floating chamber (m²). The fluxes were rejected if the Pearson
303 determination coefficient (*R*²) was below 0.9 for CO₂, below 0.85 for CH₄, and below 0.6 for N₂O.
304 Since the concentrations of CH₄ and N₂O were about 10–1000 times smaller than those of CO₂, we
305 found, similarly to Tremblay et al. (2005), that the less strict *R*² value would be justified. When the
306 flux is approaching zero, the difference between measurements will be close to the precision of the
307 instrument which results in higher share of random fluctuation in data and lower *R*². Exception was
308 made for the repeatedly measured similar low efflux concentrations of CO₂ in case of highly
309 persistent CH₄ efflux with an *R*² higher than 0.95.

310 In case of ebullition, the additional *Slope* for ebullition was calculated directly from visible
311 concentration “jumps” on the plots versus total time of floating experiments at a particular measuring

312 site (Fig.3), i.e. in case of a single ebullition event for two or more floating chamber experiments at a
313 particular measuring site, the time for ebullitive flux *Slope* calculation was gained as a sum of all
314 “on-water” experiment times. To avoid considering the ebullition due to the possible disturbance
315 created by setting up the experiment, all plots with ebullition occurring during the first three minutes
316 of floating were rejected and remeasured.

317 **3.3.2 Calculation of dissolved CO₂ values**

318 All CO₂ sensors had a fixed measuring depth, therefore we could do the depth correction for
319 each measurement time interval once for all. We assumed a constant atmospheric pCO₂ of 400 µatm
320 (<http://co2now.org/>), which was taken as the equilibrium value for the air-water interface for the
321 calculations of dissolved CO₂ saturation (DCO₂) values (Laas et al., 2016) as during the 24 h period
322 CO₂ concentrations in air are changing. For the comparison with the flux measurement, the exact
323 DCO₂ values were calculated according to measured air CO₂ concentrations (Table 3).

324 **3.3.3 Estimation of GHG emissions of the Estonian lakes**

325 We used our collected data to estimate the daily summer GHG emissions of the studied lakes.
326 We extrapolated our results further by combining the experimental data from our study with the
327 typology of Estonian lakes (Ott, 2006; ME, 2020) to present a rough estimate of GHG emissions of all
328 Estonian lakes. We assumed that lake type is affecting the summer emission of GHG from the open
329 water area. The typology utilizes physical and chemical parameters which all display large variation
330 in the study area: carbonate content of water (DIC), water humic substance (DOC) content, the
331 presence of summer stratification, size, depth, and connection with the brackish water Baltic Sea.
332 While macrophytes are not used as a classifier in the typology, the extent of macrophyte coverage
333 is nevertheless largely predicted by the lake type in the study area (Alahuhta et al., 2018), mostly
334 because of being related to depth and water optical parameters. Carbonates, humic substances,
335 stratification, and macrophytes have all been shown to affect lake GHG emissions (e.g. Tank et al.,
336 2009; Weyhenmeyer et al., 2015; Yang et al., 2015; Andrade et al., 2019b; Webb et al., 2019;
337 Andrade et al., 2020, 2021). Accordingly, our assumption is well supported by published evidence.

338 Pelagic GHG emission of a whole lake was calculated by multiplying the average GHG
339 emissions in $\text{mg m}^{-2} \text{ day}^{-1}$ by the lake surface area. To compare the warming effect on climate of these
340 three GHGs, it is reasonable to convert all the emissions into CO₂ equivalents (denoted in tables 4–5
341 as CO₂e) by weighing the amount of the different gases with their Global Warming Potential (GWP).
342 We used the GWP coefficient of 1 for CO₂, 28 for CH₄, and 265 for N₂O based on the lifetime of 100
343 years without feedback (Myhre et al., 2013).

344 To estimate the GHG emissions from all 2536 Estonian lakes, average type specific emissions
345 of CO₂ and CH₄ in $\text{mg m}^{-2} \text{ day}^{-1}$ were multiplied by the total area of lakes belonging to that type. We
346 decided to leave N₂O out from the final balance, as we considered the precision of our instrument
347 insufficient for measuring prevailing very small fluxes in the lakes. The environmental data register of
348 Estonia (EDR) was used for calculating the type specific total areas of lakes. For the lakes with
349 unidentified type in the EDR (1345 of total 2536), if possible, we assigned a type by using known
350 physico-chemical parameters (Information System of Environmental Monitoring) in combination with
351 soil and landscape type published in Estonian Geoportal (GP). In special cases, the Estonian name of
352 the lake was used as a hint for the lake type, e.g. lakes with names including ‘allik-’ (spring), ‘laugas-
353 ‘ or ‘lauka-’ (marsh pool), and ‘-laht’ or ‘lahe-’ (bay) in certain landscape areas were designated to
354 Alk, DarkSoft, and Coastal type, respectively. The remaining area of lakes with unidentified type
355 (1.7% of total lake area and 14% of the pooled area of small lakes, *i.e.*, excluding Large and V-
356 Large), was divided among types proportionally with the areal division of the small lakes with known
357 types excluding Coastal. The area of Narva Reservoir (106 km²) was added to Lake Peipsi (V-Large)
358 since it is fed by waters from this lake whereas only the Estonian parts of both water bodies (shared
359 with Russia) were added to the calculations.

360 **3.4 Statistical analysis**

361 The fluxes of CO₂ and CH₄ were compared with physical, chemical, and biological variables
362 (DCO₂, DO, pH, water temperature, lake size, mean and maximum depth, depth at sampling site,
363 metalimnion depth, TP, TN, N:P ratio, Chl *a*, DOC, HCO₃⁻, K_d, Secchi depth, phytoplankton biomass,
364 air temperature and pressure, wind speed) by means of pairwise linear (Pearson) correlation. As

365 Coastal deviated in water salinity and specific conductance from all the other lakes by about an order
366 of magnitude, we used Spearman rank correlation to study the relationships of these two variables and
367 their water column gradients with the fluxes of CO₂ and CH₄.

368

369 **4. Results**

370 **4.1 Environmental parameters**

371 The maximum depth of the studied lakes ranged from 1 to 25 m with three lakes being more
372 than 10 m deep (Table 2). During our field campaign, the three deepest lakes displayed stable
373 stratification with anoxic hypolimnion while Alk, albeit shallow, showed well developed thermal
374 stratification with fully oxygenated hypolimnion. The depth profiles of temperature, salinity, pH,
375 DCO₂, and DO are presented on Fig. 4. TP levels were indicative to rather high eutrophication in all
376 lakes except Alk, while the opposite was true for TN (Table 2), and all inorganic nutrients NO₃-N,
377 NH₄-N, and PO₄-P remained below 1 mg L⁻¹ in most of the lakes (see Table S1 for more detail). The
378 hypolimnia of LightSoft and StratAlk were also rich in reduced nitrogen (Table S1). Water sulphates
379 content varied from 2 mg L⁻¹ to 32 mg L⁻¹ with the exception of Coastal, which had sulphates level as
380 high as 266 mg L⁻¹ at the time of our experiments (Table S1).

381 **4.2 Fluxes of CO₂, CH₄, and N₂O**

382 Based on the R² of flux calculations (linear regression of the gas concentrations in the
383 chamber headspace versus time), we omitted two nonlinear declines of N₂O from DarkSoft and
384 StratAlk with R²<0.6, where the readings of N₂O in the chamber air decreased by 0.04–0.05 ppm(v)
385 during the first 5 minutes of chamber incubation and levelled off subsequently. For the rest of the
386 measurements with low R² values, the change in N₂O concentrations was less than 0.04 ppm(v)
387 during the incubation time. We consider this to be too close to the detection limit of our instrument for
388 quantitative conclusions, and we interpret these measurements hereafter as very small fluxes that we
389 cannot confirm to differ from zero (Fig. 5).

390 Our results demonstrate a broad variety of CO₂ fluxes among the lakes (Figs 5 and 6, Table 4)
391 with the most active emissions from Alk, StratAlk, and DarkSoft and with negative fluxes in Coastal,

392 V-Large, and LightSoft. As expected, the fluxes correlated strongly with surface DCO_2 values in lakes
393 (Table S2). The strong correlation with Secchi depth must be taken cautiously since among the two
394 most transparent waterbodies, Alk was the most active CO_2 emitter and Coastal the most active
395 binder.

396 By CH_4 emissions, Coastal was the most active, followed by LightSoft, StratAlk, and Alk
397 (Figs 5 and 6, Table 4). The first three lake types were also emitting bubbles with the same order of
398 activity. CH_4 fluxes displayed strong correlation with CO_2 saturation differences between the lakes'
399 surface and metalimnion (Table S2). CH_4 emissions also correlated with the salinity and/or specific
400 conductance depth gradients (increases towards bottom) in water (Table S2). Both CO_2 and CH_4
401 fluxes correlated weakly with pH and TN; in case of CO_2 , both correlations were negative.

402 We observed measurable N_2O emission only in Alk (Fig. 5, Table 4). It is worth mentioning
403 that Alk displayed very high $\text{NO}_3\text{-N}$ levels (3.13 mg L^{-1} compared to $0.03 \pm 0.04 \text{ mg L}^{-1}$ in other
404 lakes) as well as the lowest TP content ($9 \mu\text{g L}^{-1}$ against $91 \pm 68 \mu\text{g L}^{-1}$) and the highest N/P mass
405 ratio (38 against 12 ± 6). A weak uptake of N_2O was recorded in Coastal and DarkSoft lake types
406 (Fig. 5, Table 4). In all the other cases, N_2O fluxes were negligible.

407 **4.3 Total GHG fluxes of Estonian lakes**

408 Regarding summer GHG fluxes, Estonian lakes were net sinks of CO_2 , and a negative net
409 balance was observed also for the sum of CO_2 and CH_4 (Table 5). The main reason here is the areal
410 dominance of the V-Large Lake Peipsi which individually remained a net sink even after considering
411 the GWP coefficients. Still, after converting the CH_4 emissions from the small lakes into CO_2
412 equivalents (CO_{2e}), the net GHG emission from Estonian lakes turned strongly positive.

413 We included the N_2O emissions in the regional balance calculations only for the three lake
414 types for which we had reliable quantitative estimates. Considering the N_2O fluxes, the GHG balance
415 increased by 11% for Alk lakes and decreased by 10% and 0.6% for DarkSoft and Coastal lakes,
416 respectively (Table 5).

417

418 **5. Discussion**

419 **5.1 General patterns**

420 We found largely variable GHG emissions in lakes located in close vicinity in a spatially
421 confined area (Estonia) but belonging to different lake types *sensu* WFD lake typology. The average
422 (\pm standard deviation) CO₂ emission of 1070 ± 2275 mg m⁻² d⁻¹ in our study is comparable with the
423 previous recordings from lakes of boreal and temperate regions (Huttunen et al., 2003; Schrier-Ujil et
424 al., 2011; Tadonleke et al., 2011). However, the lakes larger than 1 km² in our study had notably
425 lower emission rates compared to Swedish and Norwegian lakes sized between 1 and 100 km² (Yang
426 et al., 2015) and the Finnish large lakes with size > 100 km² (Rantakari and Kortelainen, 2005). Our
427 average CH₄ emission of 114 ± 207 mg m⁻² d⁻¹ was notably high, likely because of the very high
428 emissions from LightSoft and Coastal lakes, as our median CH₄ emission of 33 mg m⁻² d⁻¹ is in good
429 accordance with other studies from the boreal region (Huttunen et al., 2003; Rasilo et al., 2015; Yang
430 et al., 2015). Our measured N₂O range is comparable with the other studies from the region (Huttunen
431 et al., 2003; Yang et al., 2015).

432 The well-known fact is that CH₄ is mostly released by sediments. Judging upon the CO₂
433 profiles (Fig. 4), lake sediments were likely also an important CO₂ source in our study in summer
434 (Laas et al., 2016; Rantakari and Kortelainen, 2005), with the exception of Alk where the main source
435 of high CO₂ is predominant calcareous ground water feeding (Laas et al., 2016). Lakes highest in
436 carbonates (Alk, StratAlk) or DOC (DarkSoft) were the strongest emitters of CO₂. As expected, the
437 correlation between DCO₂ in the surface layer and CO₂ fluxes was very strong (Table S2), suggesting
438 DCO₂ as a very good predictor for the flux. Laas et al. (2016) has demonstrated clear negative
439 correlation between the gradient of DCO₂ and the trophic state of the lake. Thus, DCO₂ and the
440 associated emission of CO₂ in the studied lakes were likely affected by an interaction of many factors:
441 the carbonate content of water (e.g. Li et al., 2021), sediment and water column catabolic activity (e.g.
442 Jonsson et al., 2003), phytoplankton and macrophyte photosynthesis (Rööm et al., 2014; Andrade et
443 al., 2021; Trolle et al., 2012), and the aeration of water by mixing (Laas et al., 2016; Andrade et al.,
444 2019b). The logical sequence of fluxes activity according to the trophic state and carbonate content in
445 our studied lake types would be as Alk – StratAlk – StartMedAlk – MedAlk – LightSoft. In other four

446 lake types, CO₂ fluxes seem to be triggered by other characteristics, for example by high water
447 column turbulence in Large and V-Large lake types or by high concentrations of organic carbon in
448 DarkSoft and Coastal.

449 With the exception of Coastal, shallow unstratified lakes were rather low CH₄ emitters
450 compared to stratified lakes. One possible explanation might be better oxygenation of sediment
451 surface in several large and shallow unstratified lakes (Fig. 4). This does not always imply more
452 efficient methanotrophy. Notably, as methanotrophy has been shown to require certain
453 undersaturation of oxygen (Thottathil et al., 2019) and is often limited by substrate (Duc et al., 2010),
454 one important factor reducing methane emissions in these well-oxygenated lakes may have been the
455 competition of aerobic sediment respiration with methanogenesis for the organic matter in surface
456 sediments. The observed positive correlation between the DCO₂ difference between the surface and
457 metalimnion and the emissions of CH₄ could result from the organic carbon content in sediments
458 affecting both variables. Opposite to CO₂, CH₄ emissions were slightly positively related to TN
459 content in water. All major CH₄-emitting lake types – Coastal, LightSoft, and StratAlk – are nutrient-
460 and organic-rich with fast metabolism, likely to build up sediment layers with high organic matter
461 content. This is in accordance with the previous studies relating the increased CH₄ emission to
462 eutrophication (Huttunen et al., 2003; Bastviken et al., 2004).

463 The lack of measurable N₂O emission in most lakes in our study is likely following the
464 seasonal dynamics of N cycling. Lake water N₂O concentrations in late summer may be at their
465 lowest due to (1) the high primary production and (2) the strongest stratification at this time.
466 Nitrification and denitrification are considered the main sources for N₂O in lakes (Seitzinger and
467 Kroeze, 1998). Both in unstratified lakes and in the epilimnia of stratified lakes, the late summer N
468 availability may be insufficient for either nitrification or denitrification to occur as phytoplankton
469 outcompetes bacteria for nitrous substrates (Webb et al., 2019). Indeed, we saw very low nitrate levels
470 in the mixed layers of all lakes except the strongly P limited Alk lake type, suggesting N limitation as
471 a reason for the possible N₂O undersaturation. Thermal stratification of lakes has also proven to be an
472 important factor in their N₂O metabolism. In the start of summer stratification in dimictic lakes, there

473 may be enough oxygen and nitrates available to curb the N₂O reduction, which is the most oxygen-
474 sensitive step of denitrification (Richardson et al., 2009), leading to the build-up of N₂O in the
475 hypolimnion. As the stratification continues, oxygen will be gradually used up and the bottom water
476 becomes increasingly reduced. By late summer, near-bottom anoxia may have lasted long enough to
477 deplete the nitrate pool and favour N₂O reduction. Indeed, many studies have found a strong seasonal
478 gradient in summer N₂O saturation in lakes and reservoirs with the N₂O peak in June and the lowest
479 and often negative flux values occurring in late summer (Knowles et al., 1981; Jacinthe et al., 2012;
480 Beaulieu et al., 2014; McCarthy et al., 2016).

481 **5.2 Individual features of lakes**

482 The studied Alk lake was intense CO₂ and moderate CH₄ emitter. As described in Laas et al.
483 (2016), the main feature that makes Alk distinct is the predominant ground water feeding of this lake
484 type while the watershed is located in carbonate-rich karstic area. Carbonate-rich ground water (> 300
485 mg L⁻¹ of HCO₃⁻, Information System of Environmental Monitoring) releases CO₂ via intense calcite
486 precipitation (Marcé et al., 2015; Laas et al., 2016) that forms the most likely source of the
487 outstanding CO₂ emissions in Alk which were comparable to the average emission of 6703 mg m⁻² d⁻¹
488 from an 1- year-old reservoir in the boreal Canada (Tadonleke et al., 2011) and surpassed 3- to 30-
489 fold the average emissions measured for the other 15 lakes and 7 – 35 years old reservoirs in that
490 study, as well as the other reports for boreal lakes (Huttunen et al., 2003; Yang et al., 2015). The low
491 TP water of the lake is highly transparent revealing almost no planktonic life forms in the water
492 column (Table 2), and most of the DCO₂ gradient is caused by diffusional efflux. These lakes behave
493 as “CO₂-chimneys” and contribute to the Estonian net CO₂ emissions equally to the other emitting
494 lake types despite of a magnitude smaller net area. In our study, the diffuse CH₄ emission in Alk
495 varied from moderate to high. The most probable source is the constantly undisturbed sediment, as the
496 lake is small and sheltered from winds, and the water column is very stable. Also, the abundant *Chara*
497 community covering most of the bottom may have reinforced CH₄ diffusional efflux to the water
498 column. Notable N₂O emission distinguishes Alk from the other studied lakes. This feature may be
499 related to the water NO₃-N levels that were by at least one order of magnitude higher than in the other

500 lakes. In fact, midsummer undersaturation of N_2O has been observed in lakes with water NO_3-N
501 content below 1 mg L^{-1} (Jacinthe et al., 2012), a threshold which was surpassed only by Alk in our
502 study. Nitrate content of water has been shown to predict N_2O emissions also in several other studies
503 (McCrackin and Elser, 2010; Webb et al., 2019). Even more, well oxygenated lakes as Alk have been
504 turned out to be net N_2O sources even at low nitrate levels as such lakes may lack a relevant
505 functional sink for N_2O (Salk and Ostrom, 2019). Due to the apparent P limitation, also the NH_4-N
506 concentration in the water is relatively high. Thus, the N_2O emitted from Alk may have been
507 produced both by aerobic nitrification in the whole water column or by denitrification at the sediment
508 chemocline.

509 The watershed of the studied StratAlk lake includes mainly sandy and loamy areas. The lake
510 has springs but also an inflowing groundwater fed stream. Because of higher phosphorus content and
511 phytoplankton activity, the lake is more eutrophic than Alk (hypertrophic for TP). Still, the content of
512 carbonates is only slightly smaller compared to Alk and the CO_2 emission levels are clearly distinct
513 from StratMedAlk to which type these lakes are usually categorised. As for Alk, the most likely
514 source may have been calcite precipitation (Marcé et al., 2015). Stable stratification most likely
515 prevented the release of CO_2 from the anoxic hypolimnion (Andrade et al., 2020). At the same time,
516 more active photosynthesis in the epilimnion, indicated by Chl *a*, pH, and O_2 saturation profiles, may
517 have been the cause for lower DCO_2 and CO_2 emissions in StratAlk compared to Alk despite the
518 comparable water carbonate levels in these lakes. In StratAlk, the CH_4 emission was the third highest.
519 Clear evidence of ebullition was observed and measured during the second experiment while the
520 diffusional flux of CH_4 was moderate. Interestingly, the bottom layer was fully depleted of NO_3-N
521 indicating the most prominent denitrification in the hypolimnion among the stratified lakes in our
522 study. The extent to which such depletion may affect the emission of N_2O from the lake probably
523 depends on the conditions in the epilimnion and/or the chemocline mixing rates (Heiskanen et al.,
524 2014). While it seems that the flux of N_2O from the epilimnion to depleted hypolimnion can turn a
525 lake into a net sink for N_2O , in other cases, despite the undersaturation in the hypolimnion, the
526 epilimnion may still act as a N_2O source (Knowles et al., 1981; Webb et al., 2019; but see Mengis et

527 al., 1997). In the present case, no epilimnetic N₂O production could be expected as the epilimnion of
528 StratAlk was depleted of both NO₃⁻ and NH₄⁺. Moreover, the sharp initial decline in N₂O
529 concentrations recorded during our chamber measurements may indicate a fast uptake of N₂O by this
530 lake, but higher precision methods would be needed to confirm this hypothesis.

531 Both CO₂ and CH₄ fluxes of studied MedAlk lake were slightly positive and higher on the
532 second measurement with higher wind speed. The mean values of 108 and 11.7 ppm m⁻² d⁻¹ for CO₂
533 and CH₄ fluxes, respectively, remained below average compared with the other studies from the
534 Nordic region. For example, average CO₂ and CH₄ emissions of 771.3 and 31.9 ppm m⁻² d⁻¹,
535 respectively, were recorded for oligotrophic and mesotrophic Norwegian and Swedish lakes with
536 surface area of 1 – 100 km² (Yang et al., 2015), and 767 and 33.3 ppm m⁻² d⁻¹ of CO₂ and CH₄,
537 respectively, for eutrophic Finnish lakes and reservoirs (Huttunen et al., 2003). High nutrient content
538 supports high phytoplankton biomass and Chl *a*, but the photosynthetic activity seems to be still the
539 minor component of the CO₂ flux balance compared to respiration, and as a result, the net flux
540 remains positive. The low CH₄ emission may be related to the large and shallow bathymetry of the
541 lake which apparently causes the low stability of the water column: DO dropped at the sediment
542 surface during our first sampling at the wind speed of 5.1 m s⁻¹, while at the second sampling with the
543 higher wind speed of 10.3 m s⁻¹, high DO zone reached the muddy surface sediment layer (Fig. 4).
544 Thus, the oxygenation of the sediment may enable high CH₄ consumption during its diffusion from
545 sediments (Thottathil et al., 2019), as well as suppress methanogenesis in the upper sediment layer
546 consisting the highest quality organic matter (Jarrell, 1985; Yang et al., 2017).

547 In the deep and stratified StratMedAlk, the nutrient content and phytoplankton biomass are
548 considerably lower compared to MedAlk, while DO is below the saturation level even in the surface
549 layer. Although CO₂ emission stayed below the average values measured in Scandinavian studies
550 (Huttunen et al., 2003; Yang et al., 2015), it still exceeded the emissions from MedAlk despite similar
551 alkalinity and DOC. The emission of CH₄ resembled closely the Scandinavian lakes (Huttunen et al.,
552 2003; Yang et al., 2015). Low DO and Chl *a* indicate strong heterotrophy in epilimnion as a possible
553 source of CO₂. Based on the measured DCO₂ gradient and the absence of DO below thermocline we

554 can assume substantial storage of both CO₂ and CH₄ in the hypolimnion (Fig. 4). As the lake is
555 relatively large, wind-induced fluctuations in the depth of thermocline and related leakage of CO₂ and
556 CH₄ from hypolimnion may thus also be possible (Huotari et al., 2011; Heiskanen et al., 2014).

557 The DarkSoft lake was the second highest CO₂ emitter of the study whereas the CH₄ emission
558 was the second lowest. With its hypertrophic nature, it is not the most common dystrophic lake, but
559 still quite representative for the post-soviet landscapes of Estonia (Ott and Kõiv, 1999). Compared to
560 the other lakes, the pH was remarkably variable during the measurements suggesting that the lack of
561 stabilising carbonate buffer was influencing the results, and at windy conditions pH stayed moderate
562 while in windless conditions the high respiration activity increased the acidity of the surface water
563 layer quite rapidly due to its very low carbonate content. Here, the phytoplankton biomass is strongly
564 light-limited in the dark brown water (Table 2), and the low DO levels give evidence of strong
565 heterotrophy (Cremona et al., 2016). Hence, the decomposition of high concentrations of DOC,
566 primarily the humic components in allochthonous organic matter, is apparently the main contributor
567 to the CO₂ flux. This kind of lakes form the second type of “CO₂-chimneys” in our study, where high
568 fluxes are caused by high organic C respiration rates (Cole et al., 1994; Jonsson et al., 2003). Low
569 CH₄ emission may be explained by water column methanotrophic activity observed also in other
570 humic boreal lakes (van Grinsven et al., 2021). Furthermore, as DarkSoft is one of the two lakes with
571 measurable N₂O uptake in our study, the simultaneous consumption of CH₄ and N₂O may indicate
572 active anaerobic CH₄ oxidation. This process would take advantage of the abundant humic substances,
573 which can promote the extracellular electron transfer and thus couple the anaerobic oxidation of CH₄
574 with the reduction of N₂O (Valenzuela et al., 2020).

575 The hypertrophic and low carbonate content LightSoft system was the second highest CH₄
576 source with a very high proportion of ebullitive flux, and at least a part-time CO₂ sink. Very high
577 cyanobacterial biomass, Chl *a* level, and DO supersaturation above the metalimnion during the first
578 measurement campaign, suggested that the CO₂ uptake can be likely attributed to high photosynthetic
579 activity. The small CO₂ release at the second measurement episode could be explained by strong
580 winds (up to 10 m s⁻¹) on 25–26 August 2014 causing deepening of the thermocline and bringing up

581 less oxygenated water (but still not considerably alleviating the lack of CO₂ in the epilimnion). The
582 hypertrophic lake sediment was evidently the strong bubbling source of CH₄, whereas the wind might
583 have increased the emissions during the second measurement.

584 The Large type (Vörtsjärv) was characterised by notably small fluxes of both CO₂ and CH₄.
585 As demonstrated by Rööm et al. (2014), the lake may also become a weak CO₂ sink in summer. The
586 shallowness and the large area opened to the wind balancing the partial pressures of gases between the
587 atmosphere and water, as well as the good balance between gross primary production and respiration
588 (Laas et al., 2012) results in a net CO₂ flux close to zero (Cremona et al. 2016). Also, the low CH₄
589 emission despite organic-rich sediment is likely due to the well oxygenated sediment surface enabling
590 high methanotrophy. In large lakes, wave action could induce the lateral transport of GHG from the
591 open littoral zone to the pelagic area (Hofmann et al., 2010), and this lake is characterized by rather
592 extensive zone of submerged macrophytes (18 % of the lake area); however, this likely does not
593 influence its pelagic GHG balance substantially, as CO₂ and CH₄ emissions from this zone are similar
594 to the pelagic area (Rööm et al., 2014).

595 The V-Large type (Peipsi) is also characterised by a large open area but since the lake is
596 deeper, it is less turbid compared to Large. Still, the whole water column is nearly saturated with DO.
597 Similarly to the Large, the V-Large acts as a weak CO₂ sink and CH₄ source, whereas the
598 photosynthetic activity is likely exceeding the total community respiration. The weak CH₄ emission
599 may be related to the sandy organic-poor sediment and good oxidising conditions. The lower
600 emissions of CO₂ in both Large and V-Large compared to the Finnish large lakes may rise from the
601 latter being mostly oligotrophic (Rantakari and Kortelainen, 2005), as lower trophic state predicts
602 lower CO₂ emissions (Trolle et al., 2012).

603 The Coastal system was the strongest CH₄ source and at the same time, the strongest CO₂ sink
604 among the studied lake types. By its GHG emissions, it reminded more a subtropical macrophyte lake
605 than a boreal lake (e.g. Colina et al., 2021). The lake is very shallow, fully saturated with DO and
606 transparent to the bottom. Dense *Chara* cover on the bottom is characteristic of lakes with low TP and
607 high TN. The lake is connected to the sea by Nasva River. Depending on the tide and currents, the

lake's salinity differed almost by a factor of two between the measurement campaigns and is generally more similar to that of the Baltic Sea than of all the other lakes in our study. In the Coastal type, CO₂ is concentrated in bottom waters, although the lake is typically shallow with a short water retention time. One reason for this gradient may be active methanotrophy inside the *Chara* stands (Kuivila et al., 1988; Liebner et al., 2011). Since both Chl *a* and total phytoplankton biomass were moderate and the bottom concentration of DCO₂ was clearly the highest among shallow unstratified lakes, the strong CO₂ uptake could be explained by intense photosynthesis by *Chara* (Laas et al., 2016). The highest CH₄ emissions, both by diffusion and ebullition, gave evidence of a high sediment decomposition rate in the warm environment (Duc et al., 2010; DelSontro et al., 2016), while the diffusion could be amplified by *Chara* similarly to the Alk type. Our finding does not fully agree with DelSontro et al (2016) who found that temperature increases CH₄ emissions only at high TP. Regarding N₂O uptake in this lake, higher water sulphate concentrations may facilitate sulphur cycling in the sediment and the growth of heterotrophic or autotrophic sulphur-oxidizing bacteria that can utilize N₂O as electron acceptor in the bottom redoxcline (Shao et al., 2010). Abundant CH₄ may support nitrate/nitrite-dependent anaerobic methane oxidation, competing for oxidised N species in the sediments (Ettwig et al., 2010; Cui et al., 2015).

5.3 Estimated GHG balance for all Estonian lakes

The estimated emissions of CO₂ and CH₄ from the open water area of all Estonian lakes in summer period were -69 and 36 T day⁻¹, which equals to -19 and 27 T C (tons of carbon) day⁻¹, respectively (Table 5). Accounting for the higher GWP of CH₄, the climate impact of the total emission of both gases equalled to 2720 T CO₂ equivalents per day (Table 5). Interestingly, the two largest lakes are strongly underrepresented in their climate impact compared to their areal share: while the largest Lake Peipsi (V-Large) with the areal share of 76% contributed to CO₂ exchange by a negative flux with the magnitude of 49% of all the CO₂ exchange, its contribution to climate impact, while still negative, formed only 2% of all the fluxes. The second largest, Lake Võrtsjärv (Large) with the areal share of 12% contributed 6% to the CO₂ exchange and 8% to the climate impact of

634 emissions. One factor behind the disproportionately small climate impact was the low 7%
635 contribution of both large lakes to the CH₄ efflux.

636 The most intriguing in the GHG balance of Estonian lakes is the ability of V-Large (Peipsi) to
637 bind CO₂ in late summer. This is strikingly different from the estimates by Rantakari and Kortelainen
638 (2005) for the Finnish large lakes (mean summer emission 337.7 ppm m⁻² d⁻¹ in lakes sized 100 –
639 4400 km², compared to -79.8 ppm m⁻² d⁻¹ in Lake Peipsi). It suggests that the annual net emission of
640 Peipsi might also be negative since the period of autumn CO₂ emission typically caused by die-off of
641 the planktonic community had still not begun in mid-September and high CO₂ uptake could be
642 expected again in early spring just after an emission peak typical at the ice break-up (Rõõm et al.,
643 2014). While being only a small CO₂ sink per m², due to its large surface area, Lake Peipsi had still a
644 huge influence on the total net flux from Estonian lakes, turning the total daily CO₂ emission negative.
645 By the CO₂ sink function, Peipsi was followed by the Coastal type having 48 times smaller total net
646 area compared to Peipsi but only 6 times smaller total CO₂ uptake.

647 Among the CO₂ net sources, the high areal emission from the Alk type was counterbalanced
648 by the small quantity of these lakes, and the most intense emitters at the country level were small
649 marsh pools (DarkSoft) followed by stratified alkalitrophic lakes (StratAlk), the second rarest type by
650 number of lakes but with a large surface area. Considering CH₄ emissions, the Coastal type was a real
651 outlier both per square metre and at the country level, showing values of the same magnitude as the
652 CO₂ fluxes of most other lake types. The next largest CH₄ sources at the country level were LightSoft
653 and StratAlk, both forming a small share of the total lake area but still considerably influencing the
654 total flux. On the other hand, the considerable contributions of the Large and V-Large to the country
655 budget of lakes could be attributed to their large surface areas.

656 Despite of excluding N₂O from the GHG balance of all Estonian lakes, the fluxes below our
657 detection limit may still have an important regional effect due to the high GWP of N₂O. For instance,
658 a close-to-zero flux of ±0.12 ppm (N₂O) m⁻² d⁻¹, too small to be confirmed by our method, would
659 affect the total exchange of GHG of V-Large by ±92 T (CO₂ equivalent) day⁻¹. Thus, more precise

660 quantification of the N₂O fluxes, especially from large lakes, would improve the accuracy of the
661 regional estimates.

662 Similar to most of the regional studies, we have based our estimate on the pelagic zone
663 measurements without accounting for the littoral zone, which may emit large amounts of GHG
664 depending on the type and amount of vegetation and sediment characteristics (Kankaala et al., 2005;
665 Rõõm et al., 2014). In our study region, helophytes have been shown to support high GHG emissions
666 (Rõõm et al., 2014) and may add to the pelagic GHG balance assessed by us, making our present
667 estimate more conservative.

668 Both the measurements in boreal lakes globally (Vachon et al., 2017) and the earlier
669 measurements by our group (Rõõm et al., 2014 and unpublished data) reveal strong CO₂ emissions
670 during early spring and late autumn due to the release of winter under-ice and summer hypolimnetic
671 accumulations, respectively. Therefore, the annual CO₂ emissions from many lake types could be
672 even higher than the summer estimates in the present study. This release, especially the autumn
673 release, is larger from deeper waterbodies (Ducharme-Riel et al., 2015). It has been estimated to
674 account on average for about 24 % of the annual flux in some Canadian lakes, and 29 – 46 % in large
675 Finnish lakes in different years (Rantakari and Kortelainen, 2005; Ducharme-Riel et al., 2015).
676 However, these releases may not suffice to counterbalance the cessation of gas exchange with
677 atmosphere during ice cover: median efflux values from large Finnish lakes show that daily summer
678 estimates can be on average two times higher than the daily annual estimates where seasonal
679 differences are accounted for (from data presented by Rantakari and Kortelainen, 2005). Since the
680 strong spring CO₂ emission is followed by the most active uptake during the period of fast planktonic
681 biomass burst in most of the boreal lakes, and from the fact that the largest Lake Peipsi was still a
682 carbon sink in late summer, prediction of the net annual CO₂ balance of Estonian lakes would require
683 data of finer seasonal resolution than presently available. It is probable that on an annual basis, uptake
684 would balance the emissions and turn the net CO₂ flux if not negative, then at least only moderately
685 positive. In the case of CH₄, the strong positive temperature dependence of fluxes has been
686 demonstrated (Kelly et al., 1981, Schulz et al., 1997, Yvon-Durocher et al., 2011, Rõõm et al., 2014),

687 and, therefore, the average annual daily emission of CH₄ from the most important emitter, Coastal
688 lake type, can only be smaller compared to midsummer emissions. For stratified lakes, the autumn
689 overturn is an important part of the yearly CH₄ cycle (Kankaala et al., 2006; Fernández et al., 2014),
690 thus potentially increasing the annual balance for these lake types. However, due to winter
691 methanotrophy, the annual daily emission may still be notably lower compared to the daily efflux at
692 the summer stratification period (Kankaala et al., 2006). While N₂O has been observed to build up
693 under ice (Cavaliere and Baulch, 2018), no significant release fluxes are expected at ice melt in spring
694 based on measurements from the Finnish lakes (Huttunen et al., 2003).

695 **6. Conclusions**

696 The studied lakes, representing all lake types in Estonia and most lake types in the whole
697 hemiboreal region, showed a large variety of their GHG fluxes. The strongest CO₂ sources were lakes
698 with predominantly allochthonous supplies of either mineral (carbonate rock) or organic (peat) carbon
699 – the alkalitrophic lake with spring water supply (Alk) and the dystrophic lake with high humic
700 substance content (DarkSoft), followed by stratified alkalitrophic and medium alkalinity lakes
701 (StratAlk and StratMedAlk). Three of nine types (Coastal, LightSoft, and V-Large) acted as net CO₂
702 sinks. The fluxes correlated strongly with surface DCO₂ values in lakes. Highest CH₄ emissions were
703 measured in the Coastal lake type, followed by LightSoft, StratAlk, and Alk, most of them also
704 emitting bubbles of CH₄. The Alk type was also the only late summer N₂O emitter, while Coastal and
705 DarkSoft lakes were acting as small sinks for N₂O. In other lakes, N₂O fluxes remained close to the
706 detection limit.

707 The results of our analysis suggest a predominant sink effect of Estonian lakes for CO₂ in
708 summer. However, the summer efflux of carbon in GHG was 8 T C day⁻¹, and the greenhouse effect
709 of this emission, 2720 T CO₂ equivalents per day, remains positive due to the high GWP of methane.

710 More detailed seasonal and spatial sampling, incorporation of littoral helophyte zones, and
711 higher precision measurements for N₂O would be the first scientific improvements required to
712 decrease the uncertainty of the regional estimate for Estonian lakes. Given the high GWP of this gas,

713 precise N₂O emission estimates for large lakes are advisable to adequately assess its greenhouse effect
714 in the region.

715 In this study, methanogenic lakes added the most to the regional climate warming effect.
716 Notably the Coastal lake type, despite its small areal share (1.6% of the regional lake area), was the
717 key emitter of GHG (62 % of total CH₄ emission). On the other hand, the two largest lakes with the
718 joint areal share of 1945 km² (88% of the regional lake area) showed very small climate impact and
719 even a cooling effect in case of Lake Peipsi. For climate mitigation efforts in Estonia, one important
720 target would be to protect the largest lakes from further eutrophication to maintain their low methane
721 and nitrous oxide emissions.

722 **Acknowledgements**

723 This research was inspired by GLEON (Global Lake Ecological Observatory Network) and
724 was funded by Estonian Research Council (PSG32, PUT1598, PSG10, PRG709, PRG1167, and
725 ETF8486) and the Swiss Program “Enhancing public environmental monitoring capacities”. This
726 project has received funding from the European Union’s Horizon 2020 research and innovation
727 programme under grant agreement No 951963.

728 Many thanks to Marina Borovkova at the Environmental Analysis Department, Environment
729 Agency, Republic of Estonia, as well as the Public Service of Environmental Data Register (Estonia),
730 for the newest data of Estonian lakes, lake types, and areas.

731 Special thanks to Henn Timm for supplying general knowledge about lake areas in Estonia
732 and photos of lakes Karijärv and Erastvere. Many thanks to Tiit Taaniel Kaljurand and Ivari
733 Kaljurand for supporting our fieldwork.

734 **References**

- 735 Alahuhta, J., Lindholm, M., Bove, C.P., Chappuis, E., Clayton, J., De Winton, M., Feldmann,
736 T., Ecke, F., Gacia, E., Grillas, P., Hoyer, M.V., Johnson, L.B., Kolada, A., Kosten, S., Lauridsen, T.
737 Lukács, B.A., Mjelde, M., Mormul, R.P., Rhazi, L., Rhazi, M., Sass, L., Søndergaard, M., Xu, J.,
738 Heino, J., 2018. Global patterns in the metacommunity structuring of lake macrophytes: regional
739 variations and driving factors. *Oecologia* 188, 1167–1182. <https://doi.org/10.1007/s00442-018-4294-0>
- 740 Andrade, C., Viveiros, F., Cruz, J.V., Coutinho, R., Silva, C., 2016. Estimation of the CO₂
741 flux from Furnas volcanic Lake (São Miguel, Azores). *J. Volcanol. Geotherm. Res.* 315, 51–64.
742 <https://doi.org/10.1016/j.jvolgeores.2016.02.005>
- 743 Andrade, C., Cruz, J.V., Viveiros, F., Branco, R., Coutinho, R., 2019a. CO₂ degassing from
744 Pico Island (Azores, Portugal) volcanic lakes. *Limnologica* 76, 72–81.
745 <https://doi.org/10.1016/j.limno.2019.04.001>
- 746 Andrade, C., Cruz, J.V., Viveiros, F., Coutinho, R., 2019b. CO₂ Flux from Volcanic Lakes in
747 the Western Group of the Azores Archipelago (Portugal). *Water* 11, 599.
748 <https://doi.org/10.3390/w11030599>
- 749 Andrade, C., Cruz, J.V., Viveiros, F., Coutinho, R., 2020. CO₂ emissions from Fogo
750 intracaldera volcanic lakes (São Miguel Island, Açores): A tool for volcanic monitoring. *J. Volcanol.*
751 *Geoth. Res.* 400, 106915. <https://doi.org/10.1016/j.jvolgeores.2020.106915>.
- 752 Andrade, C., Cruz, J.V., Viveiros, F., Coutinho, R., 2021. Diffuse CO₂ emissions from Sete
753 Cidades volcanic lake (São Miguel Island, Azores): Influence of eutrophication processes. *Environ.*
754 *Pollut.* 268, Part A, 115624. <https://doi.org/10.1016/j.envpol.2020.115624>.
- 755 Bastviken, D., Cole, J., Pace, M., Tranvik, L., 2004. Methane emissions from lakes:
756 dependence of lake characteristics, two regional assessments, and a global estimate. *Global*
757 *Biogeochem. Cy.* 18, GB4009. <https://doi.org/10.1029/2004GB002238>
- 758 Beaulieu, J.J., Smolenski, R.L., Nietch, C.T., Townsend-Small, A., Elovitz, M.S., Schubauer-
759 Berigan, J.P., 2014. Denitrification alternates between a source and sink of nitrous oxide in the

760 hypolimnion of a thermally stratified reservoir. *Limnol. Oceanogr.* 59, 495–506.

761 <http://dx.doi.org/10.4319/lo.2014.59.2.0495>

762 Bodelier, P.L.E., Steenbergh, A.K., 2014. Interactions between methane and the nitrogen
763 cycle in light of climate change. *Curr. Opin. Env. Sust.* 9–10, 26–36.

764 <https://doi.org/10.1016/j.cosust.2014.07.004>

765 Bogard, M.J., del Giorgio, P.A., Boutet, L., Garcia-Chaves, M.C., Prairie, Y.T., Merante, A.,
766 Derry, A.M., 2014. Oxidic water column methanogenesis as a major component of aquatic CH₄ fluxes.
767 *Nat. Commun.* 5, 5350. <https://doi.org/10.1038/ncomms6350>

768 Cavaliere, E., Baulch, H.M., 2018. Denitrification under lake ice. *Biogeochemistry* 137, 285–
769 295. <https://doi.org/10.1007/s10533-018-0419-0>

770 Chapuis-Lardy, L., Wrage, N., Metay, A., Chotte, J.-L., Bernoux, M., 2007. Soils, a sink for
771 N₂O? A review. *Global Change Biol.* 13, 1–17. <http://dx.doi.org/10.1111/j.1365-2486.2006.01280.x>

772 Cole, J.J., Caraco, N.F., Kling, G.W., Kratz, T.K., 1994. Carbon dioxide supersaturation in
773 the surface waters of lakes. *Science* 265, 1568–1570. <https://doi.org/10.1126/science.265.5178.1568>

774 Colina, M., Kosten, S., Silvera, N., Clemente, J.M., Meerhoff, M., 2021. Carbon fluxes in
775 subtropical shallow lakes: contrasting regimes differ in CH₄ emissions. *Hydrobiologia*.
776 <https://doi.org/10.1007/s10750-021-04752-1>

777 Cremona, F., Laas, A., Nõges, P., Nõges, T., 2016. An estimation of diel metabolic rates of
778 eight limnological archetypes from Estonia using high-frequency measurements. *Inland Waters* 6,
779 352–363. <https://doi.org/10.1080/IW-6.3.971>

780 Cui, M., Ma, A., Qi, H., Zhuang, X., Zhuang, G., 2015. Anaerobic oxidation of methane: an
781 “active” microbial process. *MicrobiologyOpen* 4, 1–11. [https://doi-](https://doi.org/10.1002/mbo3.232)
782 [org.ezproxy.utlib.ut.ee/10.1002/mbo3.232](https://doi.org/10.1002/mbo3.232)

783 Davidson, T.A., Audet, J., Jeppesen, E., Landkildehus, F., Lauridsen, T.L., Søndergaard, M.,
784 Syväranta, J., 2018. Synergy between nutrients and warming enhances methane ebullition from
785 experimental lakes. *Nature Clim. Change* 8, 156–160. <https://doi.org/10.1038/s41558-017-0063-z>

- 786 Del Giorgio, P.A., Cole, J.J., Caraco, N.F., Peters, R.H., 1999. Linking planktonic biomass
787 and metabolism to net gas fluxes in northern temperate lakes. *Ecology* 80, 1422–1431.
788 [https://doi.org/10.1890/0012-9658\(1999\)080\[1422:LPBAMT\]2.0.CO;2](https://doi.org/10.1890/0012-9658(1999)080[1422:LPBAMT]2.0.CO;2)
- 789 DelSontro, T., Beaulieu, J.J., Downing, J.A., 2018. Greenhouse gas emissions from lakes and
790 impoundments: Upscaling in the face of global change. *Limnol. Oceanogr.* 3, 64–75.
791 <https://doi.org/10.1002/lol2.10073>
- 792 DelSontro, T., Boutet, L., St-Pierre, A., del Giorgio, P.A., Prairie, Y.T., 2016. Methane
793 ebullition and diffusion from northern ponds and lakes regulated by the interaction between
794 temperature and system productivity. *Limnol. Oceanogr.* 61, S62–S77.
795 <https://doi.org/10.1002/lno.10335>
- 796 Downing, J.A., 2009. Global limnology: up-scaling aquatic services and processes to planet
797 Earth. *SIL Proceedings 1922-2010* 30, 1149–1166. <https://doi.org/10.1080/03680770.2009.11923903>
- 798 Duc, N.T., Crill, P., Bastviken, D., 2010. Implications of temperature and sediment
799 characteristics on methane formation and oxidation in lake sediments. *Biogeochemistry* 100, 185–
800 196. <https://doi.org/10.1007/s10533-010-9415-8>
- 801 Ducharme-Riel, V., Vachon, D., del Giorgio, P.A., Prairie, Y.T., 2015. The Relative
802 Contribution of Winter Under-Ice and Summer Hypolimnetic CO₂ Accumulation to the Annual CO₂
803 Emissions from Northern Lakes. *Ecosystems* 18, 547–559. [https://doi.org/10.1007/s10021-015-9846-](https://doi.org/10.1007/s10021-015-9846-0)
804 0
- 805 Edler, L., 1979. Recommendations for Marine Biological Studies in the Baltic Sea.
806 *Phytoplankton and Chlorophyll. Balt. Mar. Biolog. Publ.* 5, 1–38.
- 807 EDR - Public service of environmental data register (Estonia)
808 <http://register.keskkonnainfo.ee/envreg/main?list=VEE&mount=view> , in Estonian language only.
809 (accessed 20.10.2021).
- 810 [EU] European Union, 2000. Directive 2000/60/EC of the European Parliament and of the
811 council of 23 October 2000 establishing a framework for community action in the field of water
812 policy. *Off. J. L* 327, 1.71.

- 813 Ettwig, K., Butler, M., Le Paslier, D., Pelletier, E., Mangenot, S., Kuypers, M.M.M.,
814 Schreiber, F., Dutilh, B.E., Zedelius, J., de Beer, D., Gloerich, J., Wessels, H.J.C.T., van Alen, T.,
815 Luesken, F., Wu, M.L., van de Pas-Schoonen, K.T., Op den Camp, H.J.M., Janssen-Megens, E.M.,
816 Francoijs, K.-J., Stunnenberg, H., Weissenbach, J., Jetten, M.S.M., Strous, M., 2010. Nitrite-driven
817 anaerobic methane oxidation by oxygenic bacteria. *Nature* 464, 543–548. [https://doi-](https://doi-org.ezproxy.utlib.ut.ee/10.1038/nature08883)
818 [org.ezproxy.utlib.ut.ee/10.1038/nature08883](https://doi-org.ezproxy.utlib.ut.ee/10.1038/nature08883)
- 819 Fernández, J.E., Peeters, F., Hofmann, H., 2014. Importance of the Autumn Overturn and
820 Anoxic Conditions in the Hypolimnion for the Annual Methane Emissions from a Temperate Lake.
821 *Environ. Sci. Technol.* 48, 7297–7304. <https://doi.org/10.1021/es4056164>
- 822 Galloway, J.N., Aber, J.D., Erisman, J.W., Seitzinger, S.P., Howarth, R.W., Cowling, E.B.,
823 Cosby, B.J., 2003. The Nitrogen Cascade. *BioScience* 53, 341–356. [https://doi.org/10.1641/0006-](https://doi.org/10.1641/0006-3568(2003)053[0341:TNC]2.0.CO;2)
824 [3568\(2003\)053\[0341:TNC\]2.0.CO;2](https://doi.org/10.1641/0006-3568(2003)053[0341:TNC]2.0.CO;2)
- 825 GP - Geoportal, Republic of Estonia, Land Board:
826 <https://xgis.maaamet.ee/xgis2/page/app/maainfo> (accessed 20.10.2021).
- 827 Heiskanen, J.J., Mammarella, I., Haapanala, S., Pumpanen, J., Vesala, T., MacIntyre, S.,
828 Ojala, A., 2014. Effects of cooling and internal wave motions on gas transfer coefficients in a boreal
829 lake. *Tellus B* 66, 22827. <https://doi.org/10.3402/tellusb.v66.22827>
- 830 Hofmann, H., Federwisch, L., Peeters, F., 2010. Wave-induced release of methane: Littoral
831 zones as source of methane in lakes. *Limnol. Oceanogr.* 55, 1990–2000.
832 <https://doi.org/10.4319/lo.2010.55.5.1990>.
- 833 Huotari, J., Ojala, A., Peltomaa, E., Nordbo, A., Launiainen, S., Pumpanen, J., Rasilo, T.,
834 Hari, P., Vesala, T., 2011. Long-term direct CO₂ flux measurements over a boreal lake: Five years of
835 eddy covariance data. *Geophys. Res. Lett.* 38, L18401. <https://doi.org/10.1029/2011GL048753>
- 836 Huttunen, J.T., Alm, J., Liikanen, A., Juutinen, S., Larmola, T., Hammar, T., Silvola, J.,
837 Martikainen, P.J., 2003. Fluxes of methane, carbon dioxide and nitrous oxide in boreal lakes and
838 potential anthropogenic effects on the aquatic greenhouse gas emissions. *Chemosphere* 52, 609–621.
839 [https://doi.org/10.1016/S0045-6535\(03\)00243-1](https://doi.org/10.1016/S0045-6535(03)00243-1)

- 840 Information System of Environmental Monitoring: <https://kese.envir.ee> (accessed
841 16.11.2021).
- 842 Jacinthe, P.A., Filippelli, G.M., Tedesco, L.P., Raftis, R., 2012. Carbon storage and
843 greenhouse gases emission from a fluvial reservoir in an agricultural landscape. *Catena* 94, 53–63.
844 <https://doi.org/10.1016/j.catena.2011.03.012>
- 845 Jarrell, K.F., 1985. Extreme Oxygen Sensitivity in Methanogenic Archaeobacteria. *BioScience*
846 35, 298–302. <https://doi.org/10.2307/1309929>
- 847 Jonsson, A., Karlsson, J., Jansson, M., 2003. Sources of carbon dioxide supersaturation in
848 clearwater and humic lakes in northern Sweden. *Ecosystems* 6, 224–235.
849 <https://doi.org/10.1007/s10021-002-0200-y>
- 850 Juutinen, S., Alm, J., Larmola, T., Huttunen, J.T., Morero, M., Martikainen, P.J., Silvola, J.,
851 2003. Major implication of the littoral zone for methane release from boreal lakes. *Global*
852 *Biogeochem. Cy.* 17, 1117. <https://doi.org/10.1029/2003GB002105>
- 853 Kankaala, P., Huotari, J., Peltomaa, E., Saloranta, T., Ojala, A., 2006. Methanotrophic activity
854 in relation to methane efflux and total heterotrophic bacterial production in a stratified, humic, boreal
855 lake. *Limnol. Oceanogr.* 51, 1195–1204. doi: 10.4319/lo.2006.51.2.1195
- 856 Kankaala, P., Huotari, J., Tulonen, T., Ojala, A., 2013. Lake-size dependent physical forcing
857 drives carbon dioxide and methane effluxes from lakes in a boreal landscape. *Limnol. Oceanogr.* 58,
858 1915–1930. <https://doi.org/10.4319/lo.2013.58.6.1915>
- 859 Kankaala, P., Käki, T., Mäkelä, S., Ojala, A., Pajunen, H., Arvola, L., 2005. Methane efflux
860 in relation to plant biomass and sediment characteristics in stands of three common emergent
861 macrophytes in boreal mesoeutrophic lakes. *Global Change Biol.* 11, 145–153.
862 <https://doi.org/10.1111/j.1365-2486.2004.00888.x>
- 863 Karlsson, J., Jansson, M., Jonsson, A., 2007. Respiration of allochthonous organic carbon in
864 unproductive forest lakes determined by the Keeling plot method. *Limnol. Oceanogr.* 52, 603–608.
865 <https://doi.org/10.4319/lo.2007.52.2.0603>

- 866 Khan, H., Marcé, R., Laas, A., Obrador, B., 2022. The relevance of pelagic calcification in the
867 global carbon budget of lakes and reservoirs. *Limnetica* 41, 000-000.
868 <https://doi.org/10.23818/limn.41.02>
- 869 Kelly, C.A., Chynoweth, D.P., 1981. The contributions of temperature and of the input of
870 organic matter in controlling rates of sediment methanogenesis. *Limnol. Oceanogr.* 26, 891–897.
871 <https://doi.org/10.4319/lo.1981.26.5.0891>.
- 872 Knowles, R., 1982. Denitrification. *Microbiol Rev.* 46, 43–70.
873 <https://doi.org/10.1128/mr.46.1.43-70.1982>
- 874 Knowles, R., Lean, D.R.S., Chan, Y.K., 1981. Nitrous oxide concentrations in lakes:
875 Variations with depth and time. *Limnol. Oceanogr.* 26, 855–866.
876 <https://doi.org/10.4319/lo.1981.26.5.0855>
- 877 Kortelainen, P., Rantakari, M., Huttunen, J.T., Mattsson, T., Alm, J., Juutinen, S., Larmola,
878 T., Silvola, J., Martikainen, P.J., 2006. Sediment respiration and lake trophic state are important
879 predictors of large CO₂ evasion from small boreal lakes. *Glob. Change Biol.* 12, 1554–1567.
880 <https://doi.org/10.1111/j.1365-2486.2006.01167.x>
- 881 Kortelainen, P., Rantakari, M., Pajunen, H., Huttunen, J.T., Mattsson, T., Juutinen, S.,
882 Larmola, T., Alm, J., Silvola, J., Martikainen, P.J., 2013. Carbon evasion/accumulation ratio in boreal
883 lakes is linked to nitrogen, *Global Biogeochem. Cycles* 27, 363–374.
884 <https://doi.org/10.1002/gbc.20036>
- 885 Kuivila, K.M., Murray, J.W., Devol, A.H., Lidstrom, M.E., Reimers, C.E., 1988. Methane
886 cycling in the sediments of Lake Washington. *Limnol. Oceanogr.* 33, 571–581.
887 <https://doi.org/10.4319/lo.1988.33.4.0571>
- 888 Laas, A., Nõges, P., Kõiv, T., Nõges, T., 2012. High frequency metabolism study in a large
889 and shallow temperate lake revealed seasonal switching between net autotrophy and net heterotrophy.
890 *Hydrobiologia* 694, 57–74. <https://doi.org/10.1007/s10750-012-1131-z>
- 891 Laas, A., Cremona, F., Meinson, P., Rõõm, E.-I., Nõges, T., Nõges, P., 2016. Summer depth
892 distribution profiles of dissolved CO₂ and O₂ in shallow temperate lakes reveal trophic state and lake

893 type specific differences. *Sci. Total Environ.* 566–567, 63–75.

894 <https://doi.org/10.1016/j.scitotenv.2016.05.038>

895 Langenegger, T., Vachon, D., Donis, D., McGinnis, D.F., 2019. What the bubble knows: Lake
896 methane dynamics revealed by sediment gas bubble composition. *Limnol. Oceanogr.* 64, 1526–1544.

897 <https://doi.org/10.1002/lno.11133>

898 Lapierre, J.-F., Seekell, D.A., Filstrup, C.T., Collins, S.M., Emi Fergus, C., Soranno, P.A.,
899 Cheruvilil, K.S., 2017. Continental-scale variation in controls of summer CO₂ in United States lakes.
900 *J. Geophys. Res. Biogeosci.* 122, 875–885. <https://doi.org/10.1002/2016JG003525>

901 Li, J., Chen, Q., Wang, T., Wang, H., Ni, J., 2021. Hydrochemistry and nutrients determined
902 the distribution of greenhouse gases in saline groundwater. *Environ. Pollut.* 286, 117383.

903 <https://doi.org/10.1016/j.envpol.2021.117383>.

904 Liebner, S., Zeyer, J., Wagner, D., Schubert, C., Pfeiffer, E.-M., Knoblauch, C., 2011.
905 Methane oxidation associated with submerged brown mosses reduces methane emissions from
906 Siberian polygonal tundra. *J. Ecol.* 99, 914–922. <https://doi.org/10.1111/j.1365-2745.2011.01823.x>

907 Marcé, R., Obrador, B., Morguá, J.-A., Lluís Riera, J., López, P., Armengol, J., 2015.
908 Carbonate weathering as a driver of CO₂ supersaturation in lakes. *Nature Geosci.* 8, 107–111.

909 <https://doi.org/10.1038/ngeo2341>

910 McCarthy, M.J., Gardner, W.S., Lehmann, M.F., Guindon, A., Bird, D.F., 2016. Benthic
911 nitrogen regeneration, fixation, and denitrification in a temperate, eutrophic lake: Effects on the
912 nitrogen budget and cyanobacteria blooms. *Limnol. Oceanogr.* 61, 1406–1423.

913 <https://doi.org/10.1002/lno.10306>

914 McCrackin, M.L., Elser, J.J., 2010. Atmospheric nitrogen deposition influences denitrification
915 and nitrous oxide production in lakes. *Ecology* 91, 528–539. <https://doi.org/10.1890/08-2210.1>

916 [ME] Ministry of the Environment, 2020. List of surface water bodies, procedure for
917 designation of surface water bodies and territorial sea status classes, values of quality indicators for
918 ecological status classes of surface water bodies and values of quality indicators for water bodies not

- 919 included in a surface water body. Regulation from 4/24/2020 no. 19. Ministry of the Environment.
920 Riigi Teataja I, 21.04.2020, 61.
- 921 Mengis, M., Gächter, R., Wehrli, B., 1997. Sources and sinks of nitrous oxide (N₂O) in deep
922 lakes. *Biogeochemistry* 38, 281–301. <https://doi.org/10.1023/A:1005814020322>
- 923 Moss, B., Stephen, D., Alvarez, C., Becares, E., Van de Bund, W., Collings, S.E., Van Donk,
924 E., De Eyto, E., Feldmann, T., Fernandez-Alaez, C., Fernandez-Alaez, M., Franken, R.J.M., Garcia-
925 Criado, F., Gross, E.M., Gyllstrom, M., Hansson, L.A., Irvine, K., Järvalt, A., Jensen, J.P., Jeppesen,
926 E., Kairesalo, T., Kornijow, R., Krause, T., Künnap, H., Laas, A., Lille, E., Lorens, B., Luup, H.,
927 Miracle, M.R., Nõges, P., Nõges, T., Nykanen, M., Ott, I., Peczula, W., Peeters, E.T.H.M., Phillips,
928 G., Romo, S., Russell, V., Salujoe, J., Scheffer, M., Siewertsen, K., Smal, H., Tesch, C., Timm, H.,
929 Tuvikene, L., Tõnno, I., Virro, T., Vicente, E., Wilson, D., 2003. The determination of ecological
930 status in shallow lakes - a tested system (ECOFRAME) for implementation of the European Water
931 Framework Directive. *Aquat. Conserv.* 13, 507–549. <https://doi.org/10.1002/aqc.592>
- 932 Myhre, G., Shindell, D., Bréon, F.-M., Collins, W., Fuglestedt, J., Huang, J., Koch, D.,
933 Lamarque J.-F., Lee, D., Mendoza, B., Nakajima, T., Robock, A., Stephens, G., Takemura, T., Zhang,
934 H., 2013. Anthropogenic and Natural Radiative Forcing. In: Stocker, T.F., Qin, D., Plattner, G.-K.,
935 Tignor, M., Allen, S.K., Boschung, J., Nauels, A., Xia, Y., Bex, V., Midgley, P.M. (Eds.), *Climate*
936 *Change 2013: The Physical Science Basis. Contribution of Working Group I to the Fifth Assessment*
937 *Report of the Intergovernmental Panel on Climate Change.* Cambridge University Press, Cambridge,
938 United Kingdom and New York, NY, USA.
939 http://www.climatechange2013.org/images/report/WG1AR5_Chapter08_FINAL.pdf
- 940 Nõges, P., 2000. Euphotic holding capacity for optically active substances. *Geophysica* 36,
941 169–176.
- 942 Nõges, P., Nõges, T., 1998. Stratification of Estonian lakes studied during hydro optical
943 expeditions in 1995–97. *Proc. Estonian Acad. Sci. Biol. Ecol.* 47, 268–281.

- 944 Nõges, P., Tuvikene, L., 2012. Spatial and annual variability of environmental and
945 phytoplankton indicators in Võrtsjärv: implications for water quality monitoring. *Est. J. Ecol.* 61,
946 227–246. <https://doi.org/10.3176/eco.2012.4.01>
- 947 Nõges, P., Van de Bund, W., Cardoso, A.C., Heiskanen, A.-S., 2007. Impact of climatic
948 variability on parameters used in typology and ecological quality assessment of surface waters—
949 implications on the Water Framework Directive. *Hydrobiologia* 584, 373–379.
950 <https://doi.org/10.1007/s10750-007-0604-y>
- 951 Ott, I., 2006. Some principles of ecological quality classification in Estonian lakes. In: de Wit,
952 H., Skjelkvale, B.L. (Eds.), *Proceedings of the 21th Meeting of the ICP Waters Programme Task
953 Force in Tallinn, Estonia, October 17.19, 2005*. Norwegian University of Science and Technology
954 (84/2006, 8.14).
- 955 Ott, I., 2010. Pinnavee seisundi hindamine, võrdlus veekogumid ja pinnavee seisundi
956 klassipiirid bioloogiliste kvaliteedielementide järgi. *Evaluation Of Surface Waters, Reference
957 Waterbodies And The Status Of Class Boundaries By The Biological Quality Elements*. Report to
958 Estonian Ministry of the Environment. Estonian University of Life Sciences, Centre for Limnology,
959 222 pp. (in Estonian)
- 960 Ott, I., Kõiv, T., 1999. Eesti väikejärvede eripära ja muutused. *Estonian Small Lakes: Special
961 Features and Changes*. Estonian Ministry of the Environment Information Centre, Tallinn, 127 pp. (in
962 Estonian)
- 963 Rantakari, M., Kortelainen, P., 2005. Interannual variation and climatic regulation of the CO₂
964 emission from large boreal lakes. *Glob. Chang. Biol.* 11, 1368–1380. [https://doi.org/10.1111/j.1365-
965 2486.2005.00982.x](https://doi.org/10.1111/j.1365-2486.2005.00982.x)
- 966 Rasilo, T., Prairie, Y.T., Del Giorgio, P.A., 2015. Large-scale patterns in summer diffusive
967 CH₄ fluxes across boreal lakes, and contribution to diffusive C emissions. *Glob Chang Biol.* 21,1124–
968 1139. doi: 10.1111/gcb.12741

- 969 Rees, A.P., Brown, I.J., Jayakumar, A., Lessin, G., Somerfield, P.J., Ward, B.B., 2021.
970 Biological nitrous oxide consumption in oxygenated waters of the high latitude Atlantic Ocean.
971 *Commun. Earth Environ.* 2, 36. <https://doi.org/10.1038/s43247-021-00104-y>
- 972 Reinart, A., Arst, H., Nõges, P., Nõges, T., 2000. Comparison of euphotic layer criteria in
973 lakes. *Geophysica* 36, 141–159.
- 974 Richardson, D., Felgate, H., Watmough, N., Thomson, A., Baggs, E., 2009. Mitigating release
975 of the potent greenhouse gas N₂O from the nitrogen cycle – could enzymic regulation hold the key?
976 *Trends Biotechnol.* 27, 388–397. <https://doi.org/10.1016/j.tibtech.2009.03.009>
- 977 Rõõm, E.-I., Nõges, P., Feldmann, T., Tuvikene, L., Kisand, A., Teearu, H., Nõges, T., 2014.
978 Years are not brothers: two-year comparison of greenhouse gas fluxes in large shallow Lake
979 Võrtsjärv, Estonia. *J. Hydrol.* 519, 1594–1606. <https://doi.org/10.1016/j.jhydrol.2014.09.011>
- 980 Salk, K.R., Ostrom, N.E., 2019. Nitrous oxide in the Great Lakes: insights from two trophic
981 extremes. *Biogeochemistry* 144, 233–243. <https://doi.org/10.1007/s10533-019-00583-4>
- 982 Sanford, R.A., Wagner, D.D., Wu, Q., Chee-Sanford, J.C., Thomas, S.H., Cruz-García, C.,
983 Rodríguez, G., Massol-Deyá, A., Krishnani, K.K., Ritalahti, K.M., Nissen, S., Konstantinidis, K.T.,
984 Löffler, F.E., 2012. Unexpected nondenitrifier nitrous oxide reductase gene diversity and abundance
985 in soils. *P. Natl. Acad. Sci. USA* 109, 19709–19714. <https://doi.org/10.1073/pnas.1211238109>
- 986 Schulz, S., Matsuyama, H., Conrad, R., 1997. Temperature dependence of methane
987 production from different precursors in a profundal sediment (Lake Constance). *FEMS Microbiol.*
988 *Ecol.* 22, 207–213. <https://doi.org/10.1111/j.1574-6941.1997.tb00372.x>
- 989 Seitzinger, S.P., Kroeze, C., 1998. Global distribution of nitrous oxide production and N
990 inputs in freshwater and coastal marine ecosystems. *Global Biogeochem. Cy.* 12, 93–113. <https://doi.org/10.1029/97GB03657>
- 991
- 992 Shao, M.F., Zhang, T., Fang, H.H.-P., 2010. Sulphur-driven autotrophic denitrification:
993 diversity, biochemistry, and engineering applications. *Appl. Microbiol. Biotechnol.* 88, 1027–1042.
994 <https://doi.org/10.1007/s00253-010-2847-1>

- 995 Schrier-Uijl, A.P., Veraart, A.J., Leffelaar, P.A., Berendse, F., Veenendaal, E.M., 2011.
996 Release of CO₂ and CH₄ from lakes and drainage ditches in temperate wetlands. *Biogeochemistry*
997 102, 265–279. <https://doi.org/10.1007/s10533-010-9440-7>
- 998 Tadonl  k  , R.D., Marty, J., Planas, D., 2012. Assessing factors underlying variation of CO₂
999 emissions in boreal lakes vs. reservoirs, *FEMS Microbiol. Ecol.* 79, 282–297.
1000 <https://doi.org/10.1111/j.1574-6941.2011.01218.x>
- 1001 Tank, S.E., Lesack, L.F.W., Hesslein, R.H., 2009. Northern Delta Lakes as Summertime CO₂
1002 Absorbers Within the Arctic Landscape. *Ecosystems* 12, 144–157. [https://doi.org/10.1007/s10021-](https://doi.org/10.1007/s10021-008-9213-5)
1003 008-9213-5
- 1004 Thottathil, S.D., Reis, P.C.J., Prairie, Y.T., 2019. Methane oxidation kinetics in northern
1005 freshwater lakes. *Biogeochemistry* 143, 105–116. <https://doi.org/10.1007/s10533-019-00552-x>
- 1006 Toming, K., Tuvikene, L., Vilbaste, S., Agasild, H., Kisand, A., Viik, M., Martma, T., Jones,
1007 R., N  ges, T., 2013. Contributions of autochthonous and allochthonous sources to dissolved organic
1008 matter in a large, shallow, eutrophic lake with a highly calcareous catchment. *Limnol. Oceanogr.* 58,
1009 1259–1270. <https://doi.org/10.4319/lo.2013.58.4.1259>
- 1010 Tranvik, L.J., Downing, J.A., Cotner, J.B., Loiselle, S.A., Striegl, R.G., Ballatore, T.J., Dillon,
1011 P., Finlay, K., Fortino, K., Knoll, L.B., Kortelainen, P.L., Kutser, T., Larsen, S., Laurion, I., Leech,
1012 D.M., McCallister, S.L., McKnight, D.M., Melack, J.M., Overholt, E., Porter, J.A., Prairie, Y.,
1013 Renwick, W.H., Roland, F., Sherman, B.S., Schindler, D.W., Sobek, S., Tremblay, A., Vanni, M.J.,
1014 Verschoor, A.M., von Wachenfeldt, E., Weyhenmeyer, G.A., 2009. Lakes and reservoirs as regulators
1015 of carbon cycling and climate. *Limnol. Oceanogr.* 54, 2298–2314.
1016 https://doi.org/10.4319/lo.2009.54.6_part_2.2298
- 1017 Tremblay, A., Therrien, J., Hamlin, B., Wichmann, E., LeDrew, L.J., 2005. Analytical
1018 techniques for measuring fluxes of CO₂ and CH₄ from hydroelectric reservoirs and natural water
1019 bodies. In: Tremblay, A. et al. (Eds.), *Greenhouse Gas Emissions—Fluxes and Processes:*
1020 *Hydroelectric Reservoirs and Natural Environments.* Springer, New York, pp. 37–85.

- 1021 Trolle, D., Staehr, P.A., Davidson, T.A., Bjerring, R., Lauridsen, T.L., Martin Søndergaard,
1022 M., Jeppesen, E., 2012. Seasonal Dynamics of CO₂ Flux Across the Surface of Shallow Temperate
1023 Lakes. *Ecosystems* 15, 336–347. <https://doi.org/10.1007/s10021-011-9513-z>
- 1024 Utermöhl, H., 1958. Zur Vervollkommung der quantitativen Phytoplanktonmethodik. *Mitt.*
1025 *Int. Ver. Theor. Angew. Limnol.* 9,1–38.
- 1026 Vachon, D., Solomon, C.T., del Giorgio, P.A., 2017. Reconstructing the seasonal dynamics
1027 and relative contribution of the major processes sustaining CO₂ emissions in northern lakes. *Limnol.*
1028 *Oceanogr.* 62, 706–722. <https://doi.org/10.1002/lno.10454>
- 1029 Valenzuela, E.I., Padilla-Loma, C., Gómez-Hernández, N., López-Lozano, N.E., Casas-
1030 Flores, S., Cervantes, F.J., 2020. Humic Substances Mediate Anaerobic Methane Oxidation Linked to
1031 Nitrous Oxide Reduction in Wetland Sediments. *Front. Microbiol.* 11, 587.
1032 <https://doi.org/10.3389/fmicb.2020.00587>
- 1033 Van Grinsven, S., Oswald, K., Wehrli, B., Jegge, C., Zopfi, J., Lehmann, M. F., Schubert, C.
1034 J., 2021. Methane oxidation in the waters of a humic-rich boreal lake stimulated by photosynthesis,
1035 nitrite, Fe(III) and humics. *Biogeosciences* 18, 3087–3101. <https://doi.org/10.5194/bg-18-3087-2021>
- 1036 Verpoorter, C., Kutser, T., Seekell, D.A., Tranvik, L.J., 2014. A global inventory of lakes
1037 based on high-resolution satellite imagery. *Geophys. Res. Lett.* 41, 6396–6402.
1038 <https://doi.org/10.1002/2014GL060641>
- 1039 Wang, M., Houlton, B.Z., Wang, S., Ren, C., van Grinsven, H.J.M., Chen, D., Xu, J., Gu, B.,
1040 2021. Human-caused increases in reactive nitrogen burial in sediment of global lakes, *The Innovation*
1041 2, 100158. <https://doi.org/10.1016/j.xinn.2021.100158>
- 1042 Webb, J.R., Hayes, N.M., Simpson, G.L., Leavitt, P.R., Baulch, H.M., Finlay, K., 2019.
1043 Widespread nitrous oxide undersaturation in farm waterbodies creates an unexpected greenhouse gas
1044 sink. *P. Natl. Acad. Sci. USA* 116, 9814–9819. <https://doi.org/10.1073/pnas.1820389116>
- 1045 Wetzel, R.G., 2001. *Limnology. Lake and River Ecosystems*, third ed. Academic Press,
1046 London (1006 pp.).

- 1047 Weyhenmeyer, G.A., Kosten, S., Wallin, M.B., Tranvik, L.J., Jeppesen, E., Roland, F., 2015.
1048 Significant fraction of CO₂ emissions from boreal lakes derived from hydrologic inorganic carbon
1049 inputs. *Nat. Geosci.* 8, 933–936. <https://doi.org/10.1038/ngeo2582>
- 1050 Whiting, G.J., Chanton, J.P., 1996. Control of the diurnal pattern of methane emission from
1051 emergent aquatic macrophytes by gas transport mechanisms. *Aquat. Bot.* 54, 237–253.
1052 [https://doi.org/10.1016/0304-3770\(96\)01048-0](https://doi.org/10.1016/0304-3770(96)01048-0)
- 1053 Yang, H., Andersen, T., Dörsch, P., Tominaga, K., Thrane, J.-E., Hessen, D.O., 2015.
1054 Greenhouse gas metabolism in Nordic boreal lakes. *Biogeochemistry* 126, 211–225.
1055 <https://doi.org/10.1007/s10533-015-0154-8>
- 1056 Yang, W.H., McNicol, G., Teh, Y.A., Estera-Molina, K., Wood, T.E., Silver, W.L., 2017.
1057 Evaluating the classical versus an emerging conceptual model of peatland methane dynamics. *Global*
1058 *Biogeochem. Cy.* 31, 1435–1453. <https://doi.org/10.1002/2017GB005622>
- 1059 Yvon-Durocher, G., Montoya, J.M., Trimmer, M., Woodward, G., 2011. Warming alters the
1060 size spectrum and shifts the distribution of biomass in freshwater ecosystems. *Global Change Biol.*
1061 17, 1681–1694. <https://doi.org/10.1111/j.1365-2486.2010.02321.x>

Figure Legends

Figure 1. Lakes included in the present study and representing all the EU WFD lake types (and one additional type, StratAlk) in the study area, Estonia. Abbreviated WFD type names are indicated in brackets. A – Lake Peipsi (V-Large) and the portative monitoring buoy; B – Võrtsjärv (Large) with the stationary monitoring buoy; C – Transparent water of Äntu Sinijärv (Alk) with the reflection of the sky on the surface and our measurement sensors under the water; D – Lake Karijärv (StratAlk); E – Valguta Mustjärv (DarkSoft): almost no reflection of the sky even in a sunny day due to the blackish water; F – Lake Erastvere (LightSoft); G – Lake Ülemiste (MedAlk) with the portative monitoring buoy; H – Lake Saadjärv (StratMedAlk) on a windless day; I – Lake Mullutu Suurlaht (Coastal) with the FTIR gas analyser. Photos A-C, E, G-I by Eva-Ingrid Rõõm, photos D and F by Henn Timm.

Figure 2. Location of the studied lakes in Estonia.

Figure 3. Example of simultaneous occurrence of diffusive and ebullitive GHG fluxes at StratAlk on July 30th, 2014. All concentrations are presented in volumetric parts per million units. Empty red and green circles represent the floating chamber aeration before the experiment and filled circles – measurements during the floating experiment. Dashed trendlines show data used for CO₂ (green) and CH₄ (red) diffusive flux calculation. Concentration “jump” between blue circles (vertical arrow) against whole “on-water” experiment time (horizontal arrow) is used as a Slope for CH₄ ebullitive flux calculation (see Eq. (1)).

Figure 4. Measured physical and chemical parameters of the studied lakes during GHG flux evaluations with floating chamber method. The deepest measured value is taken 2-4 cm below sediment surface (except for DCO₂ measured with buoy). For a better overview,

some points (marked with black) are labelled with measured values. Note the differences in x-axis scaling in case of DCO₂ (marked with different green colours).

Figure 5. Results of the floating chamber flux measurements. A – summaries of CO₂ (green) CH₄ diffusive fluxes (red) and the ebullitive flux of CH₄ (blue) on the left scale; B - diffusive CH₄ flux presented with higher resolution on the right scale; C - measured N₂O fluxes. White columns denote very small fluxes which numeric value cannot be reliably confirmed by our method. Diagonally cut columns indicate that values exceed the scales. Column labels show the average flux values for CO₂ and ebullitive CH₄ (A), diffusive CH₄ (B), and N₂O (C). Error bars show the standard deviation (in section A separately for CO₂ and CH₄ ebullitive flux). Lakes are denoted by type as described in Table 1.

Figure 6. Distribution of lake types according to average CO₂ and CH₄ fluxes in ppm m⁻² day⁻¹.

Figure 1



Figure 2

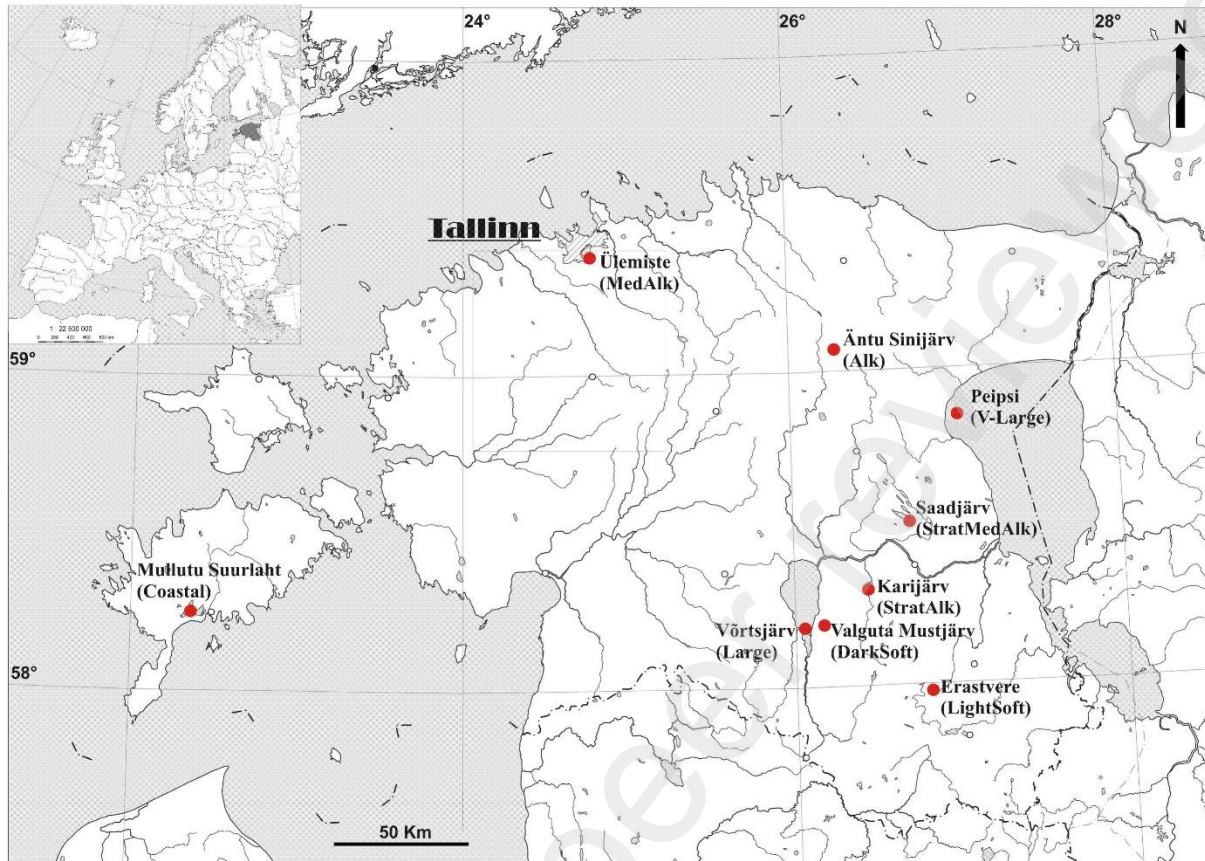


Figure 3

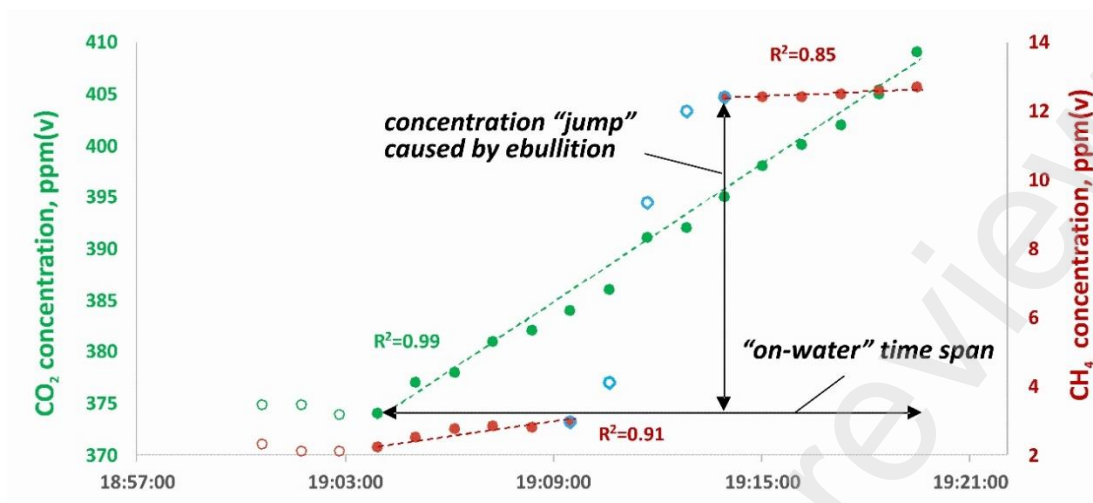


Figure 4

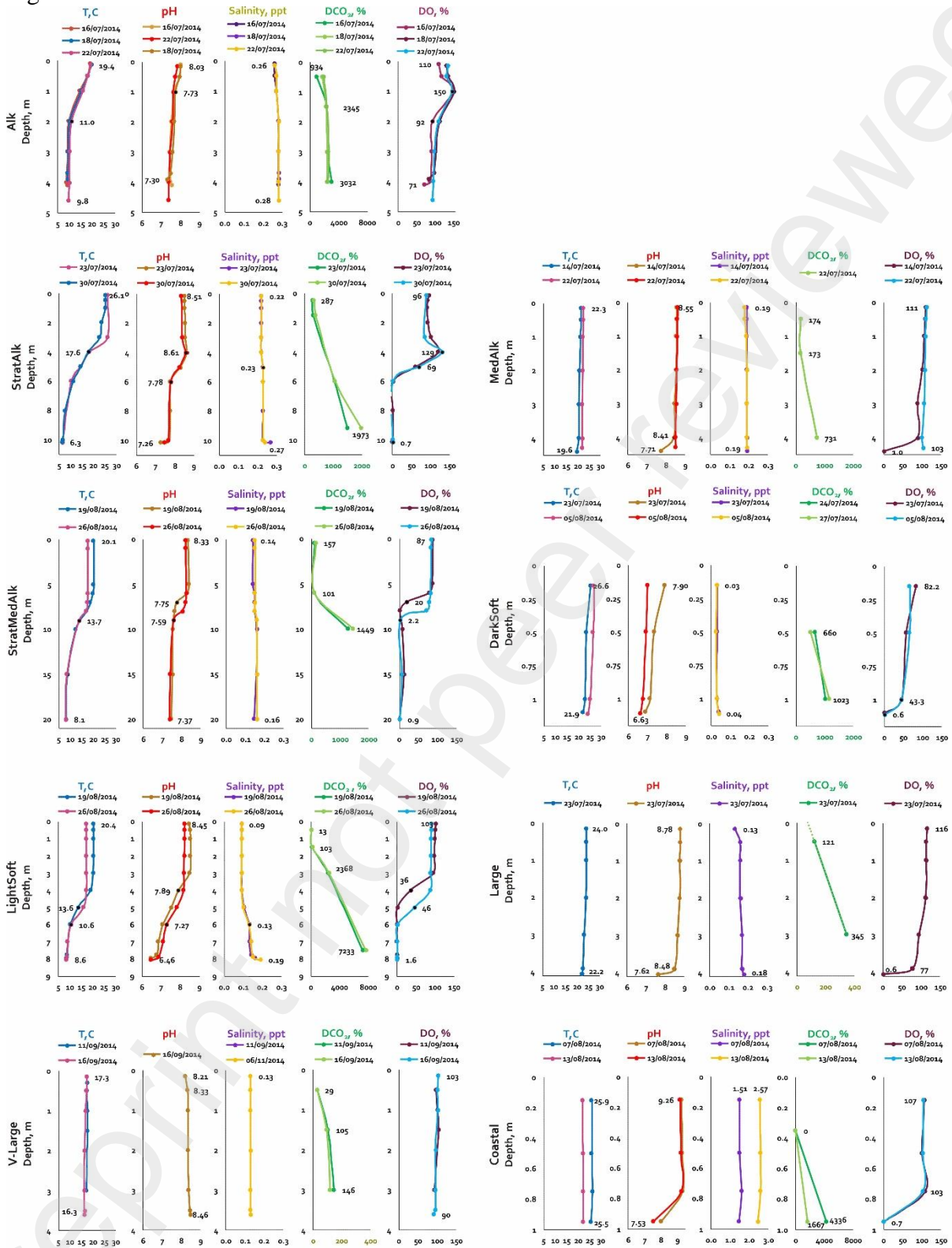


Figure 5

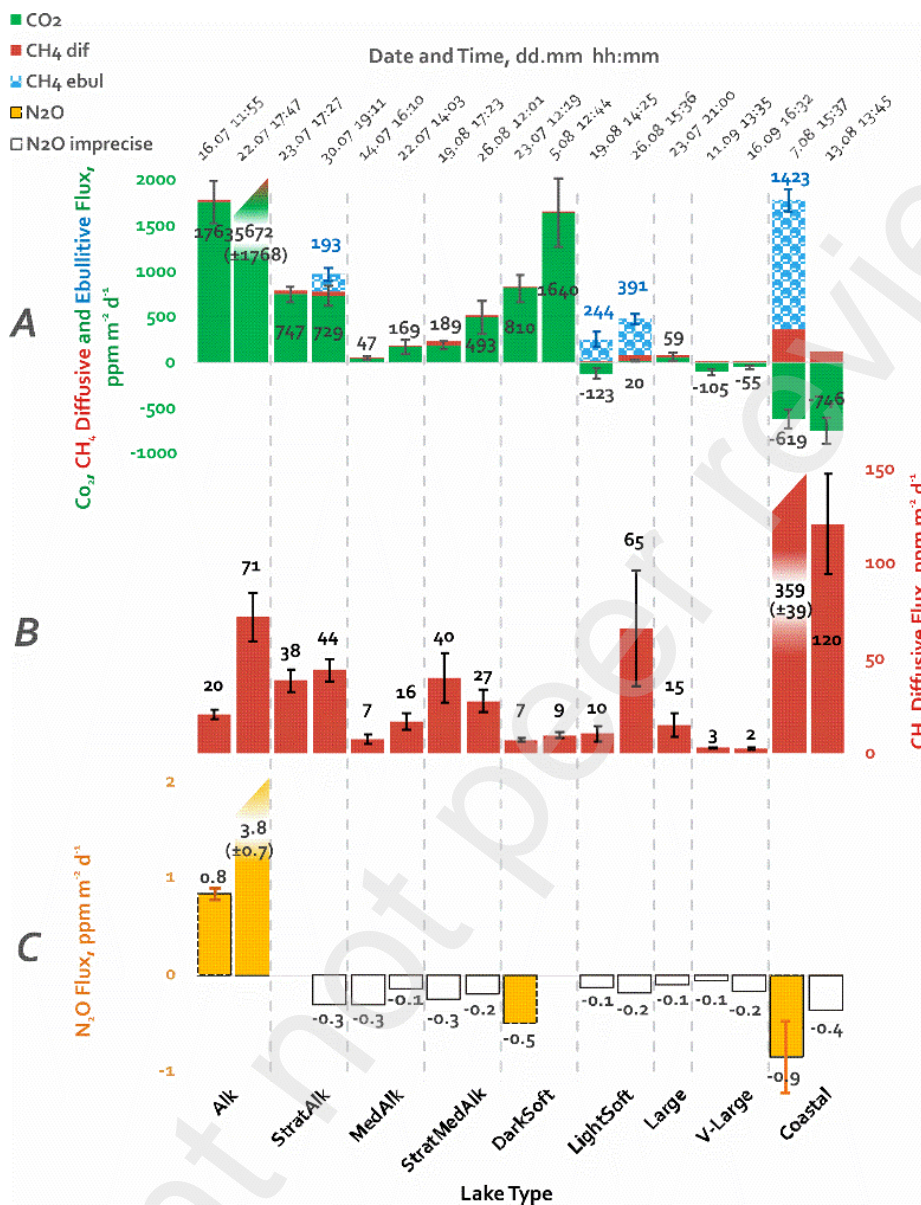


Figure 6

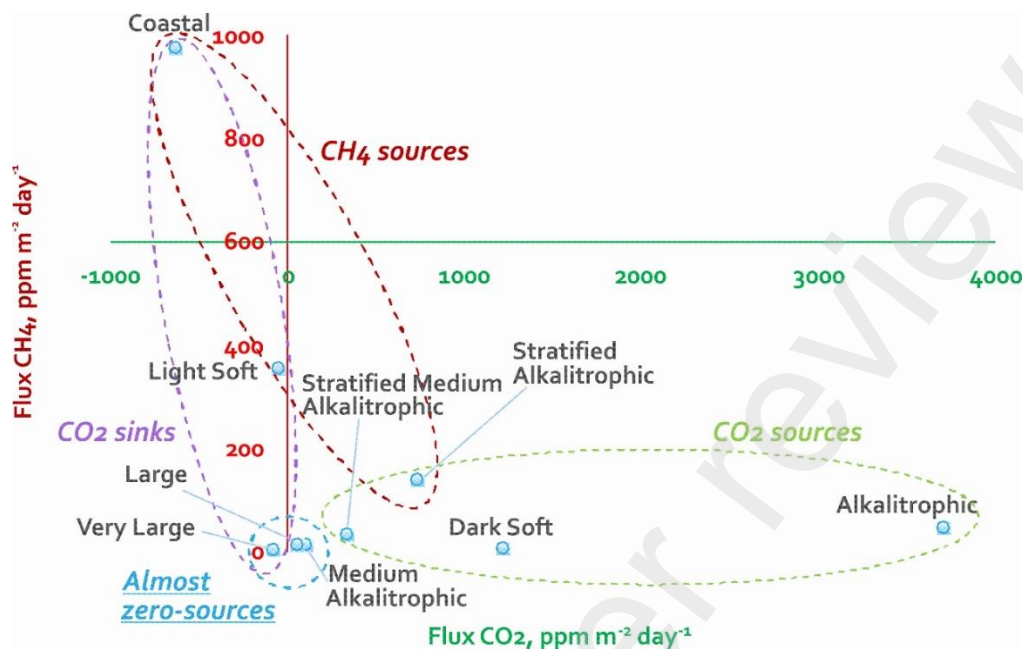


Table 1. Estonian lake types according to the European Water Framework Directive

Type name	Abbreviation	Area km ²	Alkalinity HCO ₃ ⁻ mg L ⁻¹	Conductivity μS cm ⁻¹	Cl ⁻ mg L ⁻¹	Thermal stratification	Colour Pt/Co scale	Representative in the current study
Alkalitrophic	Alk	<10	>240	> 400	<25	Non-stratified	N/A	Äntu Sinijärv
Alkalitrophic, Stratified ^a	StratAlk	<10	>240	> 400	<25	Stratified	N/A	Karijärv
Non-stratified, medium alkalinity	MedAlk	<10	80–240	165–400	<25	Non-stratified	N/A	Ülemiste
Stratified, medium alkalinity	StratMedAlk	<10	80–240	165–400	<25	Stratified	N/A	Saadjärv
Dark-coloured soft-water lakes	DarkSoft	<10	<80	<165	<25	Non-stratified	≥100°	Valguta Mustjärv
Light-coloured soft-water lakes	LightSoft	<10	<80	<165	<25	Non-stratified	<100°	Erastvere
Lake Võrtsjärv	Large	100–300	80–240	165–400	<25	Non-stratified	<100°	Võrtsjärv
Lake Peipsi	V-Large	>1000	80–240	165–400	<25	Non-stratified	<100°	Peipsi

[Type here]

Coastal lakes

Coastal

>25

Non-stratified

Mullutu Suurlaht

^a - Additional subtype separated from stratified medium alkalinity lakes

Preprint not peer reviewed

Table 2. General description of the study lakes. ^{OM} - average values of our measurements, ^{DB}- long-term average values from the database of the Centre for Limnology, Estonia. TP — total phosphorous, TN — total nitrogen, Chl a — chlorophyll a, DOC — dissolved organic carbon, HCO_3^- — alkalinity, K_d — vertical light-attenuation coefficient. # - most samples of Phytoplankton are integrated, with the exception of Saadjärv and Erastvere, where the surface water / three layers (surface/metalimnion/bottom) average samples were used. * - In case of Lake Peipsi (Peipus), only an areal share of 10489 km² is in Estonia. Phytoplankton taxonomic groups: Bac stands for diatoms, Chryso – chrysophytes, Crypto – cryptophytes, Cy – cyanobacteria, Chloro – chlorophytes, Dino – dinoflagellates.

Variable	Alk (Äntu Sinijärv)	StratAlk (Karijärv)	Medalk (Ülemiste)	StratMedalk (Saadjärv)	DarkSoft (Valguta Mustjärv)	LightSoft (Erastvere)	Large (Vörtsjärv)	V-Large (Peipsi)*	Coastal (Mullutu Suurlaht)
Trophic status ^{DB}	Alkalitrophic	Eutrophic	Eutrophic	Mesotrophic	Hypertrophic	Hypertrophic	Eutrophic	Eutrophic	Eutrophic
Mixing regime ^{DB}	Polymictic	Dimictic	Polymictic	Dimictic	Polymictic	Dimictic	Polymictic	Polymictic	Polymictic
Area (ha) ^{DB}	2.1	84	944	724.5	20.4	16.3	27000	261100	412.7
Mean depth (m) ^{DB}	6	5.7	2.5	8	<1	3.5	2.8	8.3	<1
Max depth (m) ^{DB}	8	14.5	4.2	25	1	9.7	6	12.9	1.7
TP ($\mu\text{g L}^{-1}$) ^{OM}	9	126	48	22	242	137	48	47	60
TN ($\mu\text{g L}^{-1}$) ^{OM}	3450	654	723	414	670	1126	910	375	1000
Chl a ($\mu\text{g L}^{-1}$) ^{OM}	1	13.5	24.7	5.62	23.19	125.64	35.71	13.4	9.04
DOC (mg L^{-1}) ^{OM}	4.72	11.9	13.7	9.9	35.2	12.3	11.8	12.3	18.1

[Type here]

HCO₃⁻ (mg L⁻¹)^{OM}	293	266	201	150	31	99	211	170	109
K_d (m⁻¹)^{DB}	0.25	-	3.5	0.42	10.34	2.96	2.76	1.6	0.58
Total Biomass of	0.77	3.02	25.07	5.19/ 3.41	1.12	23.60/ 11.85	8.34	7.38	8.67
Phytoplankton (g/m³)^{OM#}									
Dominant families of	<i>Bac, Chryso,</i>	<i>Cy, Dino,</i>	<i>Cy, Bac,</i>	<i>Bac, Cy,</i>	<i>Chryso, Cy,</i>	<i>Cy, Chloro,</i>	<i>Cy, Bac,</i>	<i>Cy, Bac,</i>	<i>Dino, Cy,</i>
Phytoplankton^{OM}	<i>Crypto</i>	<i>Chryso</i>	<i>Chloro</i>	<i>Chloro</i>	<i>Chloro</i>	<i>Dino</i>	<i>Chloro, Dino</i>	<i>Chloro</i>	<i>Chloro</i>
Secchi depth (m)^{OM}	8 (bottom)	4.1	0.55	4.9	0.15	1.25	0.55	2.9	1.7 (bottom)
Water residence time (y)^{DB}	7	1	0.33	0.13	0.33	0.5	1	2	0.2
Watershed size (km²)^{DB}	1,37	11.1	98.8	28.4	1,34	5.2	3116	47800	238

Table 3. Dates of experiments and weather conditions during measurements. MSt – data range (and average) of daily mean meteorological variables during measurements from the closest meteorological station to the lake, Local – data from the measuring site. Lakes are denoted by type as described in Table 1.

Lake	Sampling point coordinates	Period of buoy measurement	Dates of flux experiments	CO ₂ air, ppm	CH ₄ air, ppm	N ₂ O air, ppm	Wind speed, m s ⁻¹ MSt	Air temperature, °C MSt	Air temperature, °C Local	Wind speed, m s ⁻¹ Local	Depth, m Local	Air pressure, mBar Local
Alk	N 59°03'50.6''	15.07-	16.07; 22.07	372	1.86	0.30	1.2-3.4	17.4-19.8 (18.7)	24.2	2.6	4.4	1008.5
	E 26°14'27.0''	22.07.2014					(2.4)					
StratAlk	N 58°18'01.2''	23.07-	23.07; 30.07	373	2.07	0.28	2.5-3.4	22.6-24.7 (23.7)	26.9	2.5	10.2	1014.5
	E 26°25'00.5''	05.08.2014					(2.9)					
MedAlk	N 59°24'45.3''	16.07-	14.07; 22.07	374	1.92	0.30	1.6-2.1	20.1-22.2 (21.2)	22.3	7.7	4.4	1016
	E 24°46'34.3''	23.07.2014					(1.9)					
StratMedAlk	N 58°32'14.8''	18.08-	19.08; 26.08	369	1.73	0.31	1.7-4.1	13.0-14.3 (13.5)	17.4	7.2	21.2	996
	E 26°38'42.2''	27.08.2014					(2.6)					
DarkSoft	N 58°12'27.4''	23.07-	23.07; 5.08	375	1.91	0.30	2.5-3.4	22.6-24.7 (23.7)	27.5	1.9	1.1	1017
	E 26°08'38.0''	05.08.2014					(2.9)					
LightSoft	N 57°58'45.8''	19.08-	19.08; 26.08	369	1.85	0.30	1.4-4.4	12.4-15.7 (13.9)	17.1	6.8	7.9	993
	E 26°46'57.7''	29.08.2014					(2.8)					

[Type here]

Large	N 58°12'43.0''	23.07-					2.5-3.4					
	E 26°06'12.5''	05.08.2014	23.07	367	2.11	0.29	(2.9)	22.6-24.7 (23.7)	27.7	0.4	4.1	985
V-Large	N 58°50'27.2''	09.09-					0.6-2.8					
	E 26°58'20.6''	16.09.2014	11.09; 16.09	382	1.81	0.31	(1.3)	9.9-16.6 (13.8)	17.1	2.0	3.6	1025.5
Coastal	N 58°14'30.7''	07.08-					1.9-7.0					
	E 22°22'00.6''	14.08.2014	7.08; 13.08	372	1.97	0.29	(4.5)	17.1-21.9 (20.4)	22.5	7.6	1.0	1011.5

Preprint not peer reviewed

Table 4. Estimates of daily summer CH₄, CO₂ and N₂O emissions of the studied lakes based on average fluxes recorded on the days of observation. For N₂O, values close to detection limits are given in brackets. Lakes are denoted by type as described in Table 1. * - CO₂ equivalent calculated by applying the 100 years coefficients of Global Warming Potential (GWP) with no feedback: 1 for CO₂, 28 for CH₄, and 265 for N₂O (Myhre et al., 2013).

Lake	Flux of CO ₂ , ppm m ⁻² d ⁻¹	Flux of CH ₄ , ppm m ⁻² d ⁻¹	Flux of N ₂ O, ppm m ⁻² d ⁻¹	Flux of CO ₂ , mg m ⁻² d ⁻¹	Flux of CH ₄ , mg m ⁻² d ⁻¹	Flux of N ₂ O, mg m ⁻² d ⁻¹	CO ₂ flux per lake, kg day ⁻¹	CH ₄ flux per lake, kg day ⁻¹	N ₂ O flux per lake, kg day ⁻¹	Total CO ₂ +CH ₄ flux, mol GHG lake ⁻¹ day ⁻¹	Total CO ₂ +CH ₄ flux, kg C lake ⁻¹ day ⁻¹	Total CO ₂ +CH ₄ flux, mol CO _{2e} * lake ⁻¹ day ⁻¹	Total CO ₂ +CH ₄ flux, T CO _{2e} * lake ⁻¹ day ⁻¹	Total CO ₂ +CH ₄ +N ₂ O flux, T CO _{2e} * lake ⁻¹ day ⁻¹
Alk	3717.8	45.9	2.32	6600	29.7	4.12	139	0.6	0.1	3188	38	4237	0.2	0.2
StratAlk	737.8	137.3	(-0.32)	1310	88.8		1100	75		29653	356	155259	6.8	
MedAlk	108.2	11.7	(-0.23)	192	7.6		1813	72		45645	548	165983	7.3	
StratMedAlk	340.8	33.4	(-0.23)	605	21.6		4384	157		109379	1314	372969	16.4	
DarkSoft	1225.4	8.0	-0.53	2175	5.2	-0.95	444	1.1	-0.2	10150	122	11925	0.5	0.5
LightSoft	-51.5	355.1	(-0.15)	-91	229.8		-15	37		1996	24	65030	2.9	
Large	59.3	14.7	(-0.11)	105	9.5		28434	2561		805720	9677	5115633	225.1	
V-Large	-79.8	2.3	(-0.12)	-142	1.5		-370071	3965		-8161746	-98028	-1488676	-65.5	

[Type here]

Coastal	-631.9	972.4	-0.62	-1122	629.3	-1.10	-4630	2597	-4.5	56681	681	4427657	194.9	193.7
----------------	--------	-------	-------	-------	-------	-------	-------	------	------	-------	-----	---------	-------	-------

Preprint not peer reviewed

Table 5. Estimation of daily summer greenhouse gas (GHG) emissions from all Estonian lakes based on measured GHG emissions and division of the total lake area between types. The N₂O emissions were excluded from the estimate of the total emission due to their marginal importance and lack of reliable quantitative data for most lake types.

Type	% of total lake area in Estonia by type	Total area of lakes by type, ha	Number of lakes by type	Mean area of lakes by type, ha	Total CO ₂ emission by type, T day ⁻¹	Total CO ₂ emission by type, T C day ⁻¹	Total CH ₄ emission by type, T day ⁻¹	Total CH ₄ emission by type, T C day ⁻¹	Total N ₂ O emission by type, T day ⁻¹	Total CO _{2e} emission ^a by type, N ₂ O excluded, T day ⁻¹	Total CO _{2e} emission ^a by type, N ₂ O included, T day ⁻¹
Alk	0.1	213	94	2.3	14	4	0.06	0.05	0.01	19	21
StratAlk	1.5	3362	114	29.5	44	12	3.0	2.3		273	
MedAlk	4.3	9536	539	17.7	18	5	0.7	0.5		74	
StratMedAlk	2.3	5025	201	25.0	30	8	1.1	0.8		114	
DarkSoft	1.5	3404	890	3.8	74	20	0.2	0.2	-0.03	88	79
LightSoft	0.8	1742	310	5.6	-2	-1	4.0	3		306	
Large	12.2	26919	1	26919	28	8	2.6	2		224	
V-Large	75.7	167588	2	83794	-238	-65	2.5	1.9		-42	
Coastal	1.6	3524	221	16.0	-40	-11	22.2	16.7	-0.04	1664	1654
Total	100	220354	2536		-69	-19	36	27		2720	

^a - GHG fluxes weighed by Global Warming Potential coefficients for 100 years without feedback: 1 for CO₂, 28 for CH₄, and 265 for N₂O (Myhre et al., 2013)

[Type here]

Preprint not peer reviewed

Appendix A (Tables S1 – S2)

Supplement 1

Table S1. Chloride, sulphate, and inorganic nutrient concentrations (mg L^{-1}) in studied lakes. * - indicates values below detection limit.

Lake	Date	Sampling depth	Chlorides	Sulphates	Si	NO ₃ -N	NH ₄ -N	PO ₄ -P
Alk	22/07/2014	integrated water column	12.4	17.7	2.56	3.13	0.067	0.006
StratAlk	26/08/2014	surface	5.44	13.1	2.5	0.012	0.006	0.008
	26/08/2014	metalimnion	5.17	13.3	2.53	0.005	0.007	0.005
	26/08/2014	bottom	5.3	6.77	5.28	*	0.55	0.263
MedAlk	22/07/2014	integrated water column	8.09	31.9	0.763	*	0.028	0.005
StratMedAlk	26/08/2014	surface	10.2	22.8	0.8	*	0.015	0.011
	26/08/2014	metalimnion	19.3	24.3	1.34	*	0.025	0.005
	26/08/2014	bottom	8.35	22.3	2.77	0.124	0.036	0.005
DarkSoft	22/07/2014	integrated water column	3.18	5.21	1.56	0.127	0.013	0.184
LightSoft	26/08/2014	surface	14	2	0.189	*	0.003	0.003
	26/08/2014	metalimnion	14.1	1.93	0.192	*	0.006	0.005

[Type here]

	26/08/2014	bottom	15.8	10.9	0.685	0.027	0.542	0.2
Large	22/07/2014	integrated water column	7.2	12	3.3	*	*	0.011
V-Large	16/09/2014	integrated water column	5.46	12.55	0.456	0.004	0.018	0.015
Coastal	12/08/2014	integrated water column	very high	266	6.52	0.012	0.088	0.005

Preprint not peer reviewed

Supplement 2

Table S2. Correlations between the GHG fluxes in lakes and lake parameters. Spearman correlation coefficients are presented for relationships including salinity or specific conductance and Pearson correlation coefficients for all the other relationships. Only results with $p \leq 0.15$ are presented, results with $p \leq 0.05$ are marked in bold.

	Fluxes, ppm					
	CO ₂		CH ₄		CH ₄ Total	
	R	p	R	p	R	p
DCO ₂ Surface, %	0.99	<0.001				
ΔDCO ₂ Surface vs Metalimnion, %			0.79	0.01	0.91	0.001
pH Surface	-0.60	0.09	0.63	0.07	0.63	0.07
pH Metalimnion	-0.55	0.13	0.59	0.10	0.54	0.13
Δ _{water} Surface vs_Metalimnion, °C	0.58	0.11				
ΔSalinity Surface_Metalimnion, ppt					-0.85	0.07
ΔSalinity Surface_Bottom, ppt					-0.88	0.04
ΔSpecific Conductance Surface_Bottom, μS cm ⁻¹					-0.85	0.07
Total Nitrogen (μg L ⁻¹)	-0.56	0.12			0.596	0.09

[Type here]

Total Biomass of Phytoplankton (g/m ³) Surface	-0.52	0.15
Secchi Depth (m)	0.71	0.03

Preprint not peer reviewed